Supplement of Geosci. Model Dev., 17, 1931–1955, 2024
https://doi.org/10.5194/gmd-17-1931-2024-supplement


Geoscientific
Model Development
Open Access

*Supplement of*

# Sensitivity of the WRF-Chem v4.4 simulations of ozone and formaldehyde and their precursors to multiple bottom-up emission inventories over East Asia during the KORUS-AQ 2016 field campaign

**Kyoung-Min Kim et al.**

*Correspondence to:* Si-Wan Kim (siwan.kim@yonsei.ac.kr)

**Table list**

Table S1. The physics and chemistry schemes that are used in this study.

Table S2. The area total emissions in Eastern China (27.7-40˚N, 115-123˚E), South Korea (34.5-38˚N, 126-130˚E), and Seoul Metropolitan Area (SMA: 37.2-37.8˚N, 126.5-127.3˚E) for each emission data set in May.

Table S3. The list of MOZART species (Emmons et al., 2010)

Table S4. The list of RACM species.

Table S5. The chemical species of anthropogenic emissions used in RACM chemistry option and their mapping formulas from MOZART chemistry option that is the input format of anthro_emiss program.

Table S6. The list of SAPRC99 species (Carter, 2000).

Table S7. Comparison of surface meteorological variables from SYNOP and WRF-Chem for the KORUS-AQ campaign period. N is the number of samples. R is correlation coefficient. RMSE is root-mean-square-error.

Table S8. The mapping table from WAS to RACM VOC based on Lu et al., 2013.

Table S9. Comparison of the aircraft-based 1-minuite-interval $O_3$, $NO_2$, CO, HCHO, TOL, XYL, ETE, and ISO observations with EDV2, EDV3, and KOV5 in SMA under 2 km height for the KORUS-AQ campaign period (unit = ppb). N is the number of samples. R is correlation coefficient. RMSE is root-mean-square-error.

Table S10. Comparison of the aircraft-based 1-minuite-interval $O_3$, $NO_2$, CO, HCHO, TOL, XYL, ETE, and ISO observations with EDV2, EDV3, and KOV5 in the Chungnam region under 2 km height for the KORUS-AQ campaign period (unit = ppb). N is the number of samples. R is correlation coefficient. RMSE is root-mean-square-error.

Table S11. Comparison of the aircraft-based 1-minuite-interval $O_3$, $NO_2$, CO, and HCHO observations with EDV2, EDV3, and KOV5 in each case distinguished by Chinese contribution to $O_3$ concentration under 2 km height (unit = ppb). N is the number of samples. R is correlation coefficient. RMSE is root-mean-square-error.

Table S12. Comparison of the aircraft-based 1-minuite-interval TOL, XYL, ETE, and ISO observations with EDV2, EDV3, and KOV5 in each case distinguished by Chinese contribution to $O_3$ concentration under 2 km height. TOL, XYL, ETE, and ISO are defined in regional atmospheric chemical model (RACM) and compared with WAS based on Table S5 (unit = ppb). N is the number of samples. R is correlation coefficient. RMSE is root-mean-square-error.

Table S13. Comparison of the aircraft-based 1-minuite-interval $O_3$, $NO_2$, CO, HCHO, TOL, XYL, ETE, and ISO observations with EDV3_Ch2 and EDV3_ChKo2 in each case. The sampling number (N), mean, mean bias compared to DC-8 observations, standard deviations ($\sigma$), and correlation coefficient (R) with observations are presented (unit = ppb).

Table S14. Comparison of relative $O_3$, $NO_2$, and Ox (= $NO_2$ + $O_3$) biases with perturbed emissions based on EDGAR-HTAP v3, which is (Model – Observation)/Observation.

Table S15. Comparison of absolute $O_3$, $NO_2$, and Ox (= $NO_2$ + $O_3$) biases with perturbed emissions based on EDGAR-HTAP v3, which is (Model – Observation).

Table S16. Comparison of relative $O_3$, $NO_2$, and Ox (= $NO_2$ + $O_3$) biases with perturbed emissions based on EDGAR-HTAP v3, which is (Model – Observation)/Observation in each city; Beijing (39.4-41.1N, 115.4-117.5E), Tianjin (38.55-40.25N, 116.7-118.1E), Chengdu (30.05-31.5N, 103-105E), Chongqing (28.15-32.25N, 105.3-110.2E), Shanghai (30.7-31.5N, 120.85-122E), Hangzhou (29.2-30.6N, 118.3-120.9E), Nanjing (31.2-32.65N, 118.35-119.25E), Guangzhou (22.55-24N, 112.9-114.05E), Shenzhen (22.4-22.9N, 113.7-114.65E), SMA (37.2-37.8N, 126.5-127.3E), Wuhan (29.95-31.4N, 113.65-115.1E), and Xian (33.65-34.75N, 107.65-109.9E).

Table S17. Same as Table S16 except absolute biases (Model-Observation, unit=ppb).

**Figure list**

Figure S1. Comparison of the model surface MDA8 $O_3$ using EDGAR-HTAP v3 between with (EDV3_Fire) and without fire emissions (EDV3) at China surface observation sites during the whole campaign period (KORUS-AQ). (a) and (b) are absolute and relative differences between EDV3 and EDV3_Fire (EDV3_Fire – EDV3) respectively. The boxes represent Northern China (NOC, 38-42˚N/106-110˚E), Sichuan-Chongqing-Guizhou (SCG, 27-33˚N/103-109˚E), Pearl River Delta (PRD, 21.5-24˚N/112-115.5˚E), Southeastern China (SEC, 24-28˚N/116-120˚E), Yangtze River Delta (YRD, 30-33˚N/119-122˚E), South Korea (KOR, 34.5-38˚N/126-130˚E), North China Plain (NCP, 34-41˚N/113-119˚E), and Northeastern China (NEC, 43-47˚N/124-130˚E). NOC, NEC, and SEC are denoted by blue boxes (non-urban). NCP, SCG, PRD, YRD, and KOR are denoted by red boxes (urban).

Figure S2. Diurnal emission factors of VOC and NOx.

Figure S3. Relative ISO (isoprene) emission change from the temperature bias at the surface (unit = %).

Figure S4. Averaged surface temperature (unit: ˚C) and relative humidity (unit: %) from (a, d) ground-based observations (SYNOP) and (b, e) the weather research and forecast (WRF) model coupled with chemistry (WRF-Chem) from 1st May to 10th June for each station and countries. The differences and correlation coefficients between averaged observations and WRF-Chem are shown (c, f).

Figure S5. Comparison of PBL heights derived from the ceilometer at Yonsei University (37.564˚N, 126.935˚E) with the WRF-Chem results during the KORUS-AQ campaign period: (a) time series of planetary boundary layer height from ceilometer and WRF-Chem (unit = m), (b) scatter plot of which x axis is ceilometer and y axis is WRF-Chem PBL height, (c) comparison of diurnal variations of PBL heights from ceilometer (grey) and WRF-Chem (red) with box whisker plot.

Figure S6. Correlation coefficient (R) between observed and simulated (a-c) MDA8 O3 and (d-f) hourly O3 with (a, d) EDV2, (b, e) EDV3, and (c, f) KOV5 emissions. The observation sites with R greater than 0.6 are indicated by a black circle.

Figure S7. Simulated surface (a-c) $NO_2$ and (d-f) HCHO concentrations and (g-i) HCHO to $NO_2$ ratio (FNR) with (a, d, g) EDV2, (b, e, h) EDV3, and (c, f, i) KOV5 emissions for 14-16

LST. FNR greater than 1 is marked with black circles. The simulated $NO_2$, HCHO, and FNR are linearly interpolated to ground-based observation sites.

Figure S8. The same as Figure 3 except Ox (= $NO_2$ + $O_3$).

Figure S9. The same as Figure 4 except Ox (= $NO_2$ + $O_3$).

Figure S10. The DC-8 flight tracks on the 22nd May and 5th June.

Figure S11. Vertically averaged (a) $O_3$ and (b) CO from DC-8 (black), EDV2 (sky blue), EDV3 (blue), EDV3 with double CO emission in China (EDV3 Ch2CO) (blue dashed) and KOV5 (red) 3 in SMA under 2 km height above ground level. The 1/2 of standard deviations are represented with black whiskers in each 200m layer. The sample number is presented with magenta color on the right side of the plots.

Figure S12. The DC-8 flight tracks on the 4th, 20¬th May and 2nd, 3rd June (Local case).

Figure S13. The DC-8 flight tracks on the 22nd, 27th, 31st May (Transport case).

Figure S14. The contribution of Chinese emissions (%) to daily surface $O_3$ concentrations at Olympic Park obtained from the EDV3 simulations with/without Chinese anthropogenic emissions.

Figure S15. Vertically averaged $O_3$ from DC-8 (black), EDV2 (sky blue), EDV3 (blue), KOV5 (red), EDV3 with doubling Chinese CO and VOC emissions (dashed blue), EDV3 with doubling Korean CO and VOC emissions (dotted blue), and EDV3 with doubling Chinese and Korean CO and VOC emissions (dotted dashed blue) in Yellow Sea under 2 km height above ground level. The 1/2 of standard deviations are represented with whiskers in each 200m layer, The sample number is presented with magenta color on the right side of the plots.

Figure S16. Same as Figure 14 except that $NO_2$ is changed to Ox (= $NO_2$ + $O_3$).

Figure S17. Same as Figure 15 except that $NO_2$ is changed to Ox (= $NO_2$ + $O_3$) .

**Table S1.** The physics and chemistry schemes that are used in this study.

| **Physics** | **Scheme** | **Reference** |
|---|---|---|
| Planetary Boundary Layer (PBL) | Yonsei University Scheme (YSU) | Hong and Noh, 2006 |
| Land surface | Unified Noah Land Surface Model | Tewari et al., 2004 |
| Microphysics | Purdue Lin Scheme | Chen and Sun, 2002 |
| Cumulus parameterization | Grell 3D Ensemble | Grell, 1993<br>Grell and Devenyi, 2002 |
| **Chemistry** | **Scheme** | **Reference** |
| Photolysis | Madronich | Madronich, 1987 |
| Gas-phase chemistry | NOAA/ESRL RACM | Stokwell et al., 1997 |
| Aerosols | MADE/VBS | Ackermann et al., 1998<br>Ahmadov et al., 2012 |

**Table S2.** The area total anthropogenic emissions in Eastern China (27.7-40˚N, 115-123˚E), South Korea (34.5-38˚N, 126-130˚E), and Seoul Metropolitan Area (SMA: 37.2-37.8˚N, 126.5-127.3˚E) for each emission data set in May.

| Region | Eastern China | | | South Korea | | | SMA | | |
|---|---|---|---|---|---|---|---|---|---|
| **Species** | **EDV2** | **EDV3** | **KOV5** | **EDV2** | **EDV3** | **KOV5** | **EDV2** | **EDV3** | **KOV5** |
| | | | | | **unit = mol/s** | | | | |
| **ISO**[1] | 0.0 | 0.0 | 31.3 | 0.0 | 0.0 | 2.5 | 0.0 | 0.0 | 0.1 |
| **SO2** | 3627 | 1991 | 1648 | 183 | 349 | 165 | 18 | 92 | 10 |
| **NO** | 10063 | 9034 | 5482 | 990 | 1191 | 886 | 196 | 214 | 191 |
| **NO2** | 0 | 0 | 0 | 0 | 0 | 0 | 0 | 0 | 0 |
| **CO** | 52304 | 53183 | 48489 | 921 | 3004 | 2113 | 268 | 240 | 388 |
| **ETH** | 519 | 715 | 579 | 18 | 16 | 30 | 5 | 5 | 6 |
| **HC3** | 406 | 542 | 545 | 60 | 58 | 45 | 16 | 18 | 10 |
| **HC5** | 508 | 695 | 507 | 66 | 65 | 36 | 18 | 20 | 8 |
| **HC8** | 317 | 435 | 534 | 53 | 54 | 41 | 13 | 16 | 9 |
| **XYL** | 176 | 246 | 270 | 15 | 16 | 41 | 4 | 4 | 9 |
| **OL2** | 1144 | 1599 | 1043 | 62 | 59 | 73 | 16 | 17 | 14 |
| **OLT** | 410 | 573 | 352 | 30 | 29 | 26 | 7 | 8 | 4 |
| **OLI** | 118 | 165 | 312 | 14 | 13 | 27 | 3 | 4 | 6 |
| **TOL** | 294 | 410 | 810 | 27 | 27 | 98 | 6 | 8 | 26 |
| **CSL** | 176 | 246 | 0 | 15 | 16 | 0 | 4 | 4 | 0 |
| **HCHO** | 96 | 134 | 47 | 15 | 16 | 9 | 4 | 5 | 2 |
| **ALD** | 430 | 599 | 41 | 34 | 34 | 6 | 8 | 10 | 1 |
| **KET** | 106 | 144 | 43 | 7 | 6 | 5 | 3 | 2 | 1 |
| **ORA2** | 0 | 0 | 0 | 0 | 0 | 0 | 0 | 0 | 0 |
| **NH3** | 4065 | 6056 | 4594 | 80 | 395 | 510 | 9 | 30 | 43 |
| **SULF** | 0 | 0 | 0 | 0 | 0 | 0 | 0 | 0 | 0 |
| **Total NMVOC**[2] | 4701 | 6503 | 5115 | 418 | 408 | 439 | 107 | 122 | 96 |
| | | | | | **unit = kg/s** | | | | |
| **PM2.5** | 98.8 | 95.2 | 42.1 | 2.5 | 4.3 | 1.0 | 0.3 | 0.8 | 0.1 |
| **PM10** | 142.3 | 133.2 | 96.7 | 3.6 | 6.6 | 7.3 | 0.4 | 1.3 | 1.1 |
| **OC** | 18.0 | 16.8 | 13.7 | 0.2 | 0.4 | 1.7 | 0.0 | 0.1 | 0.1 |
| **BC** | 12.5 | 11.6 | 8.5 | 0.7 | 0.5 | 0.6 | 0.1 | 0.1 | 0.1 |

[1] Note ISO in Table S3 is only from anthropogenic sources. ISO is mainly emitted from biogenic sources using MEGAN.

[2] NMVOC is non-methane volatile organic compounds.

**Table S3**. The list of MOZART species (Emmons et al., 2010).

| Species | Atomic composition | Note |
|---|---|---|
| **ISOP** | $C_5H_8$ | isoprene |
| **SO2** | $SO_2$ | sulfur dioxide |
| **NO** | NO | nitric oxide |
| **NO2** | $NO_2$ | nitrogen dioxide |
| **CO** | CO | carbon monoxide |
| **C2H6** | $C_2H_6$ | ethane |
| **C2H5OH** | $C_2H_5OH$ | ethanol |
| **CH3OH** | $CH_3OH$ | methanol |
| **C3H8** | $C_3H_8$ | propane |
| **BIGALK** | $C_5H_{12}$ | lumped alkanes C>3 |
| **TOLUENE** | $C_6H_5(CH_3)$ | lumped aromatics |
| **C2H4** | $C_2H_2$ | ethene |
| **BIGENE** | $C_4H_8$ | lumped alkenes C>3 |
| **CH2O** | $CH_2O$ | formaldehyde |
| **CH3CHO** | $CH_3CHO$ | acetaldehyde |
| **CH3COCH3** | $CH_3COCH_3$ | acetone |
| **MEK** | $CH_3C(O)CH_2CH_3$ | methyl ethyl ketone |
| **NH3** | $NH_3$ | Ammonia |

**Table S4.** The list of RACM species.

| Species | Definition |
|---|---|
| **ISO** | Isoprene |
| **SO2** | Sulfur dioxide |
| **NO** | Nitric oxide |
| **NO2** | Nitrogen dioxide |
| **CO** | Carbon monoxide |
| **ETH** | Ethane |
| **HC3** | Alkanes, alcohols, esters, and alkynes with HO rate constant(298 K, 1 atm) less than 3.4 x $10^{-12}$ $cm^3$ $s^{-1}$ |
| **HC5** | Alkanes, alcohols, esters, and alkynes with HO rate constant(298K , 1 atm) between 3.4 x $10^{-12}$ and 6.8 x $10^{-12}$ $cm^3$ $s^{-1}$ |
| **HC8** | Alkanes, alcohols, esters, and alkynes with HO rate constant(298 K, 1 atm) greater than 6.8 x $10^{-12}$ $cm^3$ $s^{-1}$ |
| **XYL** | Xylene and more reactive aromatics |
| **OL2** | Ethene |
| **OLT** | Terminal alkenes |
| **OLI** | Internal alkenes |
| **TOL** | Toluene and less reactive aromatics |
| **CSL** | Cresol and other hydroxy substituted aromatics |
| **HCHO** | Formaldehyde |
| **ALD** | Acetaldehyde and higher aldehydes |
| **KET** | Ketones |
| **ORA2** | Acetic acid and higher acids |
| **NH3** | Ammonia |
| **SULF** | Sulfuric acid |
| **PM2.5** | Particulate matter under 2.5 μm diameter |
| **PM10** | Particulate matter under 10 μm diameter |
| **OC** | Organic carbon |
| **BC** | Black carbon |

**Table S5.** The chemical species of anthropogenic emissions used in RACM chemistry option and their mapping formulas from MOZART chemistry option that is the input format of *anthro_emiss* program.

| WRF-Chem | EDGAR-HTAP v2 (v3) | KORUS v5 |
|---|---|---|
| **RACM** | **MOZART to RACM** | **SAPRC-99 to RACM** |
| ISO | 0 | ISOP |
| SO2 | SO2 | SO2 |
| NO | NOx | NO + NO2 |
| NO2 | 0 | 0 |
| CO | CO | CO |
| ETH | C2H6[1)] | ALK1[2)] |
| HC3 | 0.5*C2H5OH[1)] + CH3OH[1)] + C3H8[1)] | ALK2[2)] + 1.11 x ALK3[2)] + 0.4 x MEOH[2)] |
| HC5 | 0.5 x BIGALK[1)] + 0.5 x C2H5OH[1)] | 0.97*ALK4[2)] |
| HC8 | 0.5 x BIGALK[1)] | ALK5[2)] |
| XYL | 0.2 x TOLUENE[1)] | ARO2[2)] |
| OL2 | C2H4[1)] | ETHE[2)] |
| OLT | 0.3 x BIGENE[1)] + C3H6[1)] | OLE1 + 0.5 x MACR + 0.5 x MVK |
| OLI | 0.4 x BIGENE[1)] | OLE2[2)] |
| TOL | 0.1 x BIGENE[1)] + 0.3 x TOLUENE[1)] | ARO1[2)] |
| CSL | 0.2 x TOLUENE[1)] | PHEN[2)] + CRES[2)] |
| HCHO | CH2O | HCHO |
| ALD | 0.2 x BIGENE[1)] + CH3CHO[1)]<br>+ 0.3 x TOLUENE[*] | CCHO[2)] + RCHO[2)] + BALD[2)] + GLY[2)]<br>+ MGLY[2)] + BACL[2)] + 0.5 x MACR[2)] |
| KET | CH3COCH3[1)] + MEK[1)] | 0.3 x ACET[2)] + 1.61 x MEK[2)] + 1.61 x PRD2[2)]<br>+ 0.5 x MVK[2)] + IPRD[2)] |
| ORA2 | 0 | 0 |
| NH3 | NH3 | NH3 |
| PM2.5 | PM2.5 | PM2.5+PMFINE |
| PM10 | PM10 | PM10 |
| OC | OC | POA |
| SULF | 0 | SULF |
| BC | BC | PEC |

[1)] Note that those are MOZART VOC species in **Table S3** (Emmons et al., 2010).

[2)] Note that those are SAPRC99 VOC species in **Table S6** (Carter, 2000).

**Table S6**. The list of SAPRC99 species (Carter, 2000).

| Species | Note |
|---|---|
| **ISOP** | Isoprene |
| **SO2** | Sulfur dioxide |
| **NO** | Nitric oxide |
| **NO2** | Nitrogen dioxide |
| **CO** | Carbon monoxide |
| **ALK1** | Alkanes and other non-aromatic compounds that react only with OH, and have kOH $< 5 \times 10^2$ ppm-1 min-1. (Primarily ethane) |
| **ALK2** | Alkanes and other non-aromatic compounds that react only with OH, and have kOH between $5 \times 10^2$ and $2.5 \times 10^3$ $ppm^{-1}$ $min^{-1}$. (Primarily propane and acetylene) |
| **ALK3** | Alkanes and other non-aromatic compounds that react only with OH, and have kOH between $2.5 \times 10^3$ and $5 \times 10^3$ $ppm^{-1}$ $min^{-1}$. |
| **ALK4** | Alkanes and other non-aromatic compounds that react only with OH, and have kOH between $5 \times 10^3$ and $1 \times 10^4$ $ppm^{-1}$ $min^{-1}$. |
| **ALK5** | Alkanes and other non-aromatic compounds that react only with OH, and have kOH greater than $1 \times 10^4$ $ppm^{-1}$ $min^{-1}$ |
| **ARO1** | Aromatics with kOH $< 2 \times 10^4$ $ppm^{-1}$ $min^{-1}$. |
| **ARO2** | Aromatics with kOH $> 2 \times 10^4$ $ppm^{-1}$ $min^{-1}$. |
| **MEOH** | Methanol |
| **ETHE** | Ethene |
| **OLE1** | Alkenes (other than ethene) with kOH $< 7 \times 10^4$ $ppm^{-1}$ $min^{-1}$. (Primarily terminal alkenes) |
| **PHEN** | Phenol |
| **CRES** | Cresols |
| **HCHO** | Formaldehyde |
| **CCHO** | Acetaldehyde and Glycolaldehyde |
| **RCHO** | Lumped C3+ Aldehydes |
| **BALD** | Aromatic aldehydes (e.g., benzaldehyde) |
| **GLY** | Glyoxal |
| **MGLY** | Methyl Glyoxal |
| **BACL** | Biacetyl |
| **MACR** | Methacrolein |
| **ACET** | Acetone |
| **MEK** | Ketones and other non-aldehyde oxygenated products which react with OH radicals slower than $5 \times 10^{-12}$ $cm^3$ $molec^{-2}$ $sec^{-1}$ |
| **PRD2** | Ketones and other non-aldehyde oxygenated products which react with OH radicals faster than $5 \times 10^{-12}$ $cm^3$ $molec^{-2}$ $sec^{-1}$ |
| **MVK** | Methyl Vinyl Ketone |
| **IPRD** | Lumped isoprene product species |
| **NH3** | Ammonia |

**Table S7.** Comparison of surface meteorological variables from SYNOP and WRF-Chem for the KORUS-AQ campaign period. N is the number of samples. R is correlation coefficient. RMSE is root-mean-square-error.

| **Nation** | | **Eastern China (sites = 271)** | | | **South Korea (sites = 48)** | | |
|---|---|---|---|---|---|---|---|
| **Variable** | | **Temperature (˚C)** | **Relative humidity (%)** | **Wind speed (m/s)** | **Temperature (˚C)** | **Relative humidity (%)** | **Wind speed (m/s)** |
| **N** | | 83698 | 83696 | 79595 | 14948 | 14946 | 14103 |
| **Mean** | **Obervation** | 20.13 | 65.02 | 2.87 | 18.94 | 65.81 | 2.56 |
| | **WRF-Chem** | 19.22 | 65.35 | 4.12 | 17.23 | 71.35 | 3.84 |
| **R** | | 0.90 | 0.85 | 0.55 | 0.88 | 0.76 | 0.62 |
| **Mean bias** | | -0.91 | 0.32 | 1.25 | -1.71 | 5.54 | 1.27 |
| **RMSE** | | 3.20 | 13.94 | 2.45 | 2.84 | 15.88 | 2.31 |

**Table S8.** The mapping table from WAS to RACM VOC based on Lu et al., 2013.

| RACM | WAS |
|---|---|
| TOL | **Toluene**, Benzene, Ethylbenzene, i-Propylbenzene, n-Propylbenzene |
| XYL | **m/p-Xylene**, **o-Xylene**, 1-3-5-Trimethylbenzene, 1-2-4-Trimethylbenzene, 1-2-3-Trimethylbenzene, 4-Ethyltoluene |
| ETE | Ethene |
| ISO | Isoprene |

**Table S9.** Comparison of the aircraft-based 1-minuite-interval $O_3$, $NO_2$, CO, HCHO, TOL, XYL, ETE, and ISO observations with EDV2, EDV3, and KOV5 in SMA under 2 km height for the KORUS-AQ campaign period (unit = ppb). N is the number of samples. R is correlation coefficient. RMSE is root-mean-square-error.

| Species | Type | N | Mean | Bias | σ | R |
|---|---|---|---|---|---|---|
| $O_3$ | **OBS** | 1081 | 80.9 | | 21.6 | |
| | **EDV2** | | 64.0 | -16.9 | 16.3 | 0.61 |
| | **EDV3** | | 66.6 | -14.2 | 16.3 | 0.63 |
| | **KOV5** | | 62.7 | -18.1 | 15.4 | 0.70 |
| $NO_2$ | **OBS** | 1068 | 4.89 | | 7.53 | |
| | **EDV2** | | 5.33 | 0.44 | 7.28 | 0.81 |
| | **EDV3** | | 5.55 | 0.66 | 7.44 | 0.80 |
| | **KOV5** | | 5.34 | 0.46 | 7.56 | 0.82 |
| CO | **OBS** | 1150 | 247 | | 98 | |
| | **EDV2** | | 148 | -98 | 53 | 0.65 |
| | **EDV3** | | 151 | -96 | 49 | 0.67 |
| | **KOV5** | | 145 | -102 | 49 | 0.71 |
| HCHO | **OBS** | 1126 | 2.65 | | 1.75 | |
| | **EDV2** | | 1.89 | -0.76 | 1.24 | 0.84 |
| | **EDV3** | | 1.99 | -0.66 | 1.32 | 0.82 |
| | **KOV5** | | 1.86 | -0.78 | 1.26 | 0.85 |
| TOL | **OBS** | 328 | 3.12 | | 1.71 | |
| | **EDV2** | | 0.63 | -2.49 | 0.43 | 0.38 |
| | **EDV3** | | 0.78 | -2.34 | 0.57 | 0.36 |
| | **KOV5** | | 2.24 | -0.88 | 1.47 | 0.40 |
| XYL | **OBS** | 182 | 0.76 | | 0.60 | |
| | **EDV2** | | 0.31 | -0.46 | 0.25 | 0.41 |
| | **EDV3** | | 0.40 | -0.37 | 0.34 | 0.41 |
| | **KOV5** | | 0.64 | -0.12 | 0.51 | 0.45 |
| ETE | **OBS** | 870 | 0.33 | | 0.44 | |
| | **EDV2** | | 0.79 | 0.46 | 0.90 | 0.71 |
| | **EDV3** | | 0.89 | 0.56 | 1.07 | 0.73 |
| | **KOV5** | | 0.69 | 0.35 | 0.71 | 0.71 |
| ISO | **OBS** | 555 | 0.10 | | 0.11 | |
| | **EDV2** | | 0.28 | 0.17 | 0.27 | 0.40 |
| | **EDV3** | | 0.27 | 0.16 | 0.26 | 0.40 |
| | **KOV5** | | 0.26 | 0.16 | 0.26 | 0.41 |

**Table S10.** Comparison of the aircraft-based 1-minuite-interval $O_3$, $NO_2$, CO, HCHO, TOL, XYL, ETE, and ISO observations with EDV2, EDV3, and KOV5 in the Chungnam region under 2 km height for the KORUS-AQ campaign period (unit = ppb). N is the number of samples. R is correlation coefficient. RMSE is root-mean-square-error.

| Species | Type | N | Mean | Bias | σ | R |
|---|---|---|---|---|---|---|
| $O_3$ | **OBS** | 560 | 101.6 | | 17.1 | |
| | **EDV2** | | 63.5 | -38.1 | 14.3 | 0.10 |
| | **EDV3** | | 60.2 | -41.3 | 13.7 | 0.06 |
| | **KOV5** | | 62.4 | -39.2 | 14.1 | 0.11 |
| $NO_2$ | **OBS** | 557 | 3.46 | | 5.07 | |
| | **EDV2** | | 4.88 | 1.43 | 4.75 | 0.26 |
| | **EDV3** | | 8.09 | 4.63 | 6.34 | 0.30 |
| | **KOV5** | | 4.79 | 1.34 | 4.79 | 0.28 |
| CO | **OBS** | 578 | 302 | | 102 | |
| | **EDV2** | | 148 | -153 | 49 | 0.51 |
| | **EDV3** | | 157 | -145 | 37 | 0.59 |
| | **KOV5** | | 142 | -159 | 34 | 0.61 |
| HCHO | **OBS** | 579 | 4.04 | | 2.48 | |
| | **EDV2** | | 2.25 | -1.79 | 1.06 | 0.41 |
| | **EDV3** | | 2.18 | -1.86 | 1.02 | 0.39 |
| | **KOV5** | | 2.49 | -1.55 | 1.19 | 0.44 |
| TOL | **OBS** | 130 | 2.65 | | 2.36 | |
| | **EDV2** | | 0.47 | -2.18 | 0.35 | 0.13 |
| | **EDV3** | | 0.50 | -2.15 | 0.35 | 0.09 |
| | **KOV5** | | 1.17 | -1.48 | 0.81 | -0.06 |
| XYL | **OBS** | 30 | 1.20 | | 1.01 | |
| | **EDV2** | | 0.11 | -1.10 | 0.09 | 0.01 |
| | **EDV3** | | 0.14 | -1.06 | 0.10 | 0.03 |
| | **KOV5** | | 0.17 | -1.03 | 0.21 | -0.42 |
| ETE | **OBS** | 255 | 2.08 | | 4.64 | |
| | **EDV2** | | 0.53 | -1.55 | 0.50 | 0.05 |
| | **EDV3** | | 0.59 | -1.49 | 0.48 | 0.06 |
| | **KOV5** | | 0.75 | -1.33 | 0.64 | 0.10 |
| ISO | **OBS** | 101 | 0.06 | | 0.06 | |
| | **EDV2** | | 0.06 | 0.00 | 0.06 | -0.17 |
| | **EDV3** | | 0.09 | 0.04 | 0.09 | -0.10 |
| | **KOV5** | | 0.06 | 0.00 | 0.06 | -0.13 |

**Table S11.** Comparison of the aircraft-based 1-minuite-interval $O_3$, $NO_2$, CO, and HCHO observations with EDV2, EDV3, and KOV5 in each case distinguished by Chinese contribution to $O_3$ concentration under 2 km height for the KORUS-AQ campaign period (unit = ppb). N is the number of samples. R is correlation coefficient. RMSE is root-mean-square-error.

| Species | Case | Type | N | Mean | Bias | σ | R |
|---|---|---|---|---|---|---|---|
| $O_3$ | **Local** (5/4,20 , 6/2,3) | **OBS** | 1125 | 81.2 | | 15.3 | |
| | | **EDV2** | | 65.2 | -15.9 | 13.4 | 0.66 |
| | | **EDV3** | | 65.2 | -16.0 | 12.8 | 0.59 |
| | | **KOV5** | | 62.6 | -18.5 | 11.5 | 0.70 |
| | **Transport** (5/25,26 ,31) | **OBS** | 605 | 95.6 | | 19.1 | |
| | | **EDV2** | | 87.3 | -8.3 | 13.8 | 0.64 |
| | | **EDV3** | | 93.1 | -2.5 | 16.0 | 0.67 |
| | | **KOV5** | | 84.8 | -10.8 | 14.3 | 0.69 |
| $NO_2$ | **Local** (5/4,20 , 6/2,3) | **OBS** | 1066 | 2.62 | | 4.92 | |
| | | **EDV2** | | 2.57 | -0.05 | 3.45 | 0.63 |
| | | **EDV3** | | 3.51 | 0.89 | 4.39 | 0.67 |
| | | **KOV5** | | 2.34 | -0.28 | 3.62 | 0.67 |
| | **Transport** (5/25,26 ,31) | **OBS** | 591 | 1.28 | | 3.60 | |
| | | **EDV2** | | 1.89 | 0.61 | 4.45 | 0.85 |
| | | **EDV3** | | 2.34 | 1.06 | 5.02 | 0.83 |
| | | **KOV5** | | 1.67 | 0.39 | 4.47 | 0.86 |
| CO | **Local** (5/4,20 , 6/2,3) | **OBS** | 1225 | 214 | | 61.7 | |
| | | **EDV2** | | 130 | -83 | 24.9 | 0.64 |
| | | **EDV3** | | 137 | -77 | 27.7 | 0.64 |
| | | **KOV5** | | 131 | -83 | 25.0 | 0.67 |
| | **Transport** (5/25,26 ,31) | **OBS** | 651 | 345 | | 128.5 | |
| | | **EDV2** | | 209 | -136 | 60.7 | 0.59 |
| | | **EDV3** | | 209 | -135 | 61.6 | 0.58 |
| | | **KOV5** | | 201 | -143 | 57.7 | 0.58 |
| HCHO | **Local** (5/4,20 , 6/2,3) | **OBS** | 1177 | 2.43 | | 1.82 | |
| | | **EDV2** | | 1.70 | -0.73 | 0.86 | 0.49 |
| | | **EDV3** | | 1.72 | -0.71 | 0.84 | 0.48 |
| | | **KOV5** | | 1.78 | -0.65 | 0.96 | 0.54 |
| | **Transport** (5/25,26 ,31) | **OBS** | 605 | 1.70 | | 1.08 | |
| | | **EDV2** | | 1.32 | -0.38 | 0.72 | 0.74 |
| | | **EDV3** | | 1.36 | -0.34 | 0.71 | 0.73 |
| | | **KOV5** | | 1.21 | -0.49 | 0.69 | 0.72 |

**Table S12.** Comparison of the aircraft-based 1-minuite-interval TOL, XYL, ETE, and ISO observations with EDV2, EDV3, and KOV5 in each case distinguished by Chinese contribution to $O_3$ concentration under 2 km height. TOL, XYL, ETE, and ISO are defined in regional atmospheric chemical model (RACM) and compared with WAS based on Table S8 (unit = ppb). N is the number of samples. R is correlation coefficient. RMSE is root-mean-square-error.

| Species | Case | Type | N | Mean | Bias | σ | R |
|---|---|---|---|---|---|---|---|
| **TOL** | **Local** (5/4,20 , 6/2,3) | **OBS** | 170 | 1.67 | | 1.40 | |
| | | **EDV2** | | 0.35 | -1.32 | 0.25 | 0.22 |
| | | **EDV3** | | 0.42 | -1.25 | 0.35 | 0.19 |
| | | **KOV5** | | 1.14 | -0.53 | 1.00 | 0.03 |
| | **Transport** (5/25,26 ,31) | **OBS** | 72 | 1.99 | | 1.48 | |
| | | **EDV2** | | 0.49 | -1.50 | 0.37 | 0.54 |
| | | **EDV3** | | 0.59 | -1.41 | 0.50 | 0.55 |
| | | **KOV5** | | 1.64 | -0.35 | 1.42 | 0.57 |
| **XYL** | **Local** (5/4,20 , 6/2,3) | **OBS** | 77 | 0.76 | | 0.85 | |
| | | **EDV2** | | 0.13 | -0.63 | 0.17 | 0.21 |
| | | **EDV3** | | 0.18 | -0.58 | 0.24 | 0.23 |
| | | **KOV5** | | 0.26 | -0.50 | 0.40 | 0.15 |
| | **Transport** (5/25,26 ,31) | **OBS** | 30 | 0.70 | | 0.42 | |
| | | **EDV2** | | 0.28 | -0.42 | 0.22 | 0.23 |
| | | **EDV3** | | 0.37 | -0.33 | 0.30 | 0.24 |
| | | **KOV5** | | 0.60 | -0.10 | 0.48 | 0.19 |
| **ETE** | **Local** (5/4,20 , 6/2,3) | **OBS** | 535 | 0.75 | | 2.78 | |
| | | **EDV2** | | 0.44 | -0.30 | 0.51 | -0.01 |
| | | **EDV3** | | 0.52 | -0.23 | 0.66 | 0.02 |
| | | **KOV5** | | 0.49 | -0.26 | 0.49 | 0.09 |
| | **Transport** (5/25,26 ,31) | **OBS** | 290 | 0.24 | | 0.38 | |
| | | **EDV2** | | 0.37 | 0.13 | 0.60 | 0.65 |
| | | **EDV3** | | 0.39 | 0.15 | 0.70 | 0.65 |
| | | **KOV5** | | 0.31 | 0.06 | 0.51 | 0.65 |
| **ISO** | **Local** (5/4,20 , 6/2,3) | **OBS** | 352 | 0.08 | | 0.09 | |
| | | **EDV2** | | 0.16 | 0.07 | 0.20 | 0.32 |
| | | **EDV3** | | 0.17 | 0.09 | 0.20 | 0.31 |
| | | **KOV5** | | 0.16 | 0.07 | 0.20 | 0.34 |
| | **Transport** (5/25,26 ,31) | **OBS** | 76 | 0.10 | | 0.10 | |
| | | **EDV2** | | 0.18 | 0.08 | 0.19 | 0.56 |
| | | **EDV3** | | 0.19 | 0.08 | 0.18 | 0.58 |
| | | **KOV5** | | 0.17 | 0.06 | 0.17 | 0.55 |

**Table S13.** Comparison of the aircraft-based 1-minuite-interval $O_3$, $NO_2$, CO, HCHO, TOL, XYL, ETE, and ISO observations with EDV3_Ch2, EDV3_Ko2, and EDV3_ChKo2 in each case. The sampling number (N), mean, mean bias compared to DC-8 observations, standard deviations (σ), and correlation coefficient (R) with observations are presented (unit = ppb).

| Species | Case | Type | N | Mean | Bias | σ | R |
|---|---|---|---|---|---|---|---|
| $O_3$ | **Local** (5/4,20 , 6/2,3) | **EDV3_Ch2** | 1125 | 68.5 | -12.7 | 12.3 | 0.62 |
| | | **EDV3_Ko2** | | 69.6 | -11.6 | 14.7 | 0.66 |
| | | **EDV3_ChKo2** | | 72.3 | -8.9 | 14.3 | 0.68 |
| | **Transport** (5/25,26 , 6/1) | **EDV3_Ch2** | 605 | 111.0 | 15.4 | 23.4 | 0.65 |
| | | **EDV3_Ko2** | | 94.8 | -0.9 | 15.8 | 0.68 |
| | | **EDV3_ChKo2** | | 112.6 | 17.0 | 23.1 | 0.66 |
| $NO_2$ | **Local** (5/4,20 , 6/2,3) | **EDV3_Ch2** | 1066 | 3.30 | 0.68 | 4.31 | 0.68 |
| | | **EDV3_Ko2** | | 3.11 | 0.50 | 3.97 | 0.67 |
| | | **EDV3_ChKo2** | | 3.05 | 0.44 | 3.95 | 0.67 |
| | **Transport** (5/25,26 , 6/1) | **EDV3_Ch2** | 591 | 2.09 | 0.81 | 4.75 | 0.83 |
| | | **EDV3_Ko2** | | 1.90 | 0.62 | 4.30 | 0.83 |
| | | **EDV3_ChKo2** | | 1.92 | 0.64 | 4.17 | 0.84 |
| CO | **Local** (5/4,20 , 6/2,3) | **EDV3_Ch2** | 1225 | 158 | -56 | 43 | 0.68 |
| | | **EDV3_Ko2** | | 155 | -59 | 42 | 0.56 |
| | | **EDV3_ChKo2** | | 176 | -38 | 53 | 0.65 |
| | **Transport** (5/25,26 , 6/1) | **EDV3_Ch2** | 651 | 331 | -13 | 122 | 0.56 |
| | | **EDV3_Ko2** | | 217 | -128 | 63 | 0.58 |
| | | **EDV3_ChKo2** | | 339 | -6 | 122 | 0.56 |
| HCHO | **Local** (5/4,20 , 6/2,3) | **EDV3_Ch2** | 1177 | 1.82 | -0.61 | 0.87 | 0.47 |
| | | **EDV3_Ko2** | | 2.03 | -0.40 | 1.18 | 0.51 |
| | | **EDV3_ChKo2** | | 2.13 | -0.30 | 1.17 | 0.51 |
| | **Transport** (5/25,26 , 6/1) | **EDV3_Ch2** | 605 | 1.78 | 0.08 | 0.98 | 0.69 |
| | | **EDV3_Ko2** | | 1.51 | -0.19 | 1.16 | 0.70 |
| | | **EDV3_ChKo2** | | 1.94 | 0.24 | 1.33 | 0.72 |
| TOL | **Local** (5/4,20 , 6/2,3) | **EDV3_Ch2** | 170 | 0.46 | -2.33 | 0.40 | 0.09 |
| | | **EDV3_Ko2** | | 0.75 | -2.04 | 0.64 | 0.23 |
| | | **EDV3_ChKo2** | | 0.79 | -2.00 | 0.65 | 0.18 |
| | **Transport** (5/25,26 , 6/1) | **EDV3_Ch2** | 72 | 0.68 | -2.20 | 0.46 | 0.50 |
| | | **EDV3_Ko2** | | 1.05 | -1.84 | 0.95 | 0.57 |
| | | **EDV3_ChKo2** | | 1.14 | -1.75 | 0.90 | 0.55 |
| XYL | **Local** (5/4,20 , 6/2,3) | **EDV3_Ch2** | 77 | 0.19 | -0.64 | 0.25 | 0.17 |
| | | **EDV3_Ko2** | | 0.30 | -0.53 | 0.42 | 0.26 |
| | | **EDV3_ChKo2** | | 0.31 | -0.52 | 0.42 | 0.23 |
| | **Transport** (5/25,26 , 6/1) | **EDV3_Ch2** | 30 | 0.35 | -0.43 | 0.30 | 0.22 |
| | | **EDV3_Ko2** | | 0.64 | -0.13 | 0.53 | 0.25 |
| | | **EDV3_ChKo2** | | 0.61 | -0.17 | 0.53 | 0.23 |
| ETE | **Local** (5/4,20 , 6/2,3) | **EDV3_Ch2** | 535 | 0.62 | -0.13 | 0.92 | 0.00 |
| | | **EDV3_Ko2** | | 0.77 | 0.02 | 1.00 | 0.02 |
| | | **EDV3_ChKo2** | | 0.87 | 0.12 | 1.17 | 0.00 |
| | **Transport** (5/25,26 , 6/1) | **EDV3_Ch2** | 290 | 0.51 | 0.26 | 0.69 | 0.65 |
| | | **EDV3_Ko2** | | 0.63 | 0.39 | 1.26 | 0.66 |
| | | **EDV3_ChKo2** | | 0.74 | 0.50 | 1.22 | 0.67 |
| ISO | **Local** (5/4,20 , 6/2,3) | **EDV3_Ch2** | 352 | 0.17 | 0.08 | 0.20 | 0.32 |
| | | **EDV3_Ko2** | | 0.15 | 0.07 | 0.17 | 0.33 |
| | | **EDV3_ChKo2** | | 0.15 | 0.06 | 0.17 | 0.33 |
| | **Transport** (5/25,26 , 6/1) | **EDV3_Ch2** | 76 | 0.16 | 0.06 | 0.16 | 0.57 |
| | | **EDV3_Ko2** | | 0.15 | 0.05 | 0.15 | 0.57 |
| | | **EDV3_ChKo2** | | 0.14 | 0.03 | 0.14 | 0.55 |

**Table S14**. Comparison of relative $O_3$, $NO_2$, and Ox (= $NO_2$ + $O_3$) biases with perturbed emissions based on EDGAR-HTAP v3, which is (Model – Observation)/Observation.

| | Emissions | NCP | SCG | YRD | PRD | KOR | NEC | NOC | SEC |
|---|---|---|---|---|---|---|---|---|---|
| **$O_3$ bias (%)** | **EDV3** | -1% | 68% | -6% | 23% | -3% | -13% | -1% | 75% |
| | **C1** | 38% | 103% | 42% | 53% | 21% | 3% | 10% | 111% |
| | **C2** | 38% | 103% | 41% | 52% | 13% | 2% | 10% | 111% |
| | **C3** | -1% | 68% | -5% | 23% | 6% | -12% | -1% | 76% |
| | **C4** | 23% | 63% | 29% | 49% | -5% | -10% | 7% | 80% |
| | **C5** | -23% | 50% | -31% | 7% | -11% | -22% | -6% | 54% |
| | **C6** | 9% | 53% | 9% | 36% | -10% | -16% | 4% | 68% |
| | **C7** | 20% | 42% | 32% | 52% | -10% | -15% | 7% | 65% |
| **$NO_2$ bias (%)** | **EDV3** | 24% | -12% | 78% | 63% | -5% | -18% | -11% | 15% |
| | **C1** | 13% | -19% | 63% | 54% | -9% | -20% | -13% | 2% |
| | **C2** | 13% | -19% | 63% | 54% | -5% | -20% | -13% | 2% |
| | **C3** | 23% | -12% | 78% | 63% | -8% | -18% | -11% | 15% |
| | **C4** | -41% | -57% | -14% | -17% | -6% | -25% | -56% | -46% |
| | **C5** | 28% | -9% | 83% | 67% | -6% | -15% | -10% | 22% |
| | **C6** | -38% | -55% | -7% | -12% | -7% | -25% | -55% | -43% |
| | **C7** | -72% | -78% | -61% | -61% | -8% | -28% | -78% | -74% |
| **Ox bias (%)** | **EDV3** | 6% | 45% | 20% | 36% | -3% | -14% | -3% | 59% |
| | **C1** | 31% | 68% | 48% | 53% | 11% | -3% | 5% | 82% |
| | **C2** | 31% | 68% | 48% | 53% | 7% | -3% | 5% | 81% |
| | **C3** | 6% | 45% | 21% | 36% | 1% | -14% | -3% | 59% |
| | **C4** | 5% | 29% | 16% | 28% | -5% | -14% | -6% | 46% |
| | **C5** | -9% | 33% | 4% | 26% | -9% | -21% | -7% | 45% |
| | **C6** | -4% | 22% | 4% | 21% | -9% | -18% | -9% | 38% |
| | **C7** | -6% | 8% | 3% | 16% | -9% | -18% | -11% | 27% |

C1: **EDV3_ChKo2**, EDGAR-HTAP v3 with double CO and VOC emissions in China and South Korea.
C2: **EDV3_Ch2**, EDGAR-HTAP v3 with double CO and VOC emissions in China.
C3: **EDV3_Ko2**, EDGAR-HTAP v3 with double CO and VOC emissions in South Korea.
C4: **EDV3_Ch0.5NOx**, EDGAR-HTAP v3 with 50% reduction of NOx emission in China.
C5: **EDV3_Ch0.5VOC**, EDGAR-HTAP v3 with 50% reduction of VOC emission in China.
C6: **EDV3_Ch0.5NOxVOC**, EDGAR-HTAP v3 with 50% reductions of NOx and VOC emissions in China.
C7: **EDV3_Ch0.25NOx**, EDGAR-HTAP v3 with 75% reduction of NOx emission in China.

**Table S15**. Comparison of absolute $O_3$, $NO_2$, and Ox (= $NO_2$ + $O_3$) biases with perturbed emissions based on EDGAR-HTAP v3, which is (Model – Observation).

| | Emissions | NCP | SCG | YRD | PRD | KOR | NEC | NOC | SEC |
|---|---|---|---|---|---|---|---|---|---|
| **$O_3$ bias (ppb)** | **EDV3** | -0.5 | 23.6 | -2.4 | 6.4 | -1.2 | -5.2 | -0.3 | 19.6 |
| | **C1** | 16.9 | 35.5 | 16.0 | 14.7 | 8.9 | 1.1 | 4.4 | 29.0 |
| | **C2** | 16.7 | 35.5 | 15.7 | 14.6 | 5.2 | 1.0 | 4.4 | 28.9 |
| | **C3** | -0.3 | 23.6 | -2.0 | 6.5 | 2.6 | -5.1 | -0.3 | 19.8 |
| | **C4** | 10.2 | 21.9 | 11.2 | 13.6 | -2.0 | -4.2 | 3.2 | 21.0 |
| | **C5** | -10.3 | 17.3 | -11.9 | 2.0 | -4.5 | -9.1 | -2.6 | 14.1 |
| | **C6** | 3.9 | 18.2 | 3.5 | 10.2 | -4.2 | -6.4 | 1.7 | 17.7 |
| | **C7** | 9.0 | 14.6 | 12.3 | 14.5 | -4.2 | -6.0 | 2.9 | 17.0 |
| **$NO_2$ bias (ppb)** | **EDV3** | 4.1 | -1.6 | 13.4 | 8.2 | -1.2 | -2.4 | -1.3 | 1.4 |
| | **C1** | 2.4 | -2.6 | 10.8 | 6.9 | -2.0 | -2.7 | -1.6 | 0.2 |
| | **C2** | 2.4 | -2.6 | 10.8 | 6.9 | -1.1 | -2.7 | -1.6 | 0.2 |
| | **C3** | 4.1 | -1.6 | 13.4 | 8.2 | -1.9 | -2.4 | -1.3 | 1.4 |
| | **C4** | -7.2 | -7.8 | -2.5 | -2.2 | -1.5 | -3.4 | -6.6 | -4.4 |
| | **C5** | 4.9 | -1.2 | 14.2 | 8.6 | -1.3 | -2.1 | -1.2 | 2.1 |
| | **C6** | -6.6 | -7.5 | -1.2 | -1.6 | -1.6 | -3.4 | -6.6 | -4.1 |
| | **C7** | -12.7 | -10.8 | -10.5 | -7.9 | -1.8 | -3.8 | -9.3 | -7.1 |
| **Ox bias (ppb)** | **EDV3** | 3.6 | 22.0 | 11.1 | 14.6 | -2.2 | -7.6 | -1.7 | 21.0 |
| | **C1** | 19.3 | 32.9 | 26.8 | 21.6 | 7.1 | -1.5 | 2.7 | 29.2 |
| | **C2** | 19.1 | 32.9 | 26.5 | 21.5 | 4.3 | -1.6 | 2.7 | 29.1 |
| | **C3** | 3.8 | 22.0 | 11.4 | 14.6 | 0.8 | -7.4 | -1.7 | 21.2 |
| | **C4** | 3.0 | 14.1 | 8.8 | 11.3 | -3.4 | -7.6 | -3.4 | 16.4 |
| | **C5** | -5.3 | 16.2 | 2.3 | 10.6 | -5.6 | -11.2 | -3.8 | 16.2 |
| | **C6** | -2.7 | 10.6 | 2.3 | 8.5 | -5.7 | -9.8 | -4.8 | 13.4 |
| | **C7** | -3.7 | 3.8 | 1.9 | 6.6 | -5.9 | -9.7 | -6.3 | 9.8 |

**C1**: **EDV3_ChKo2**, EDGAR-HTAP v3 with double CO and VOC emissions in China and South Korea.
**C2**: **EDV3_Ch2**, EDGAR-HTAP v3 with double CO and VOC emissions in China.
**C3**: **EDV3_Ko2**, EDGAR-HTAP v3 with double CO and VOC emissions in South Korea.
**C4**: **EDV3_Ch0.5NOx**, EDGAR-HTAP v3 with 50% reduction of NOx emission in China.
**C5**: **EDV3_Ch0.5VOC**, EDGAR-HTAP v3 with 50% reduction of VOC emission in China.
**C6**: **EDV3_Ch0.5NOxVOC**, EDGAR-HTAP v3 with 50% reductions of NOx and VOC emissions in China.
**C7**: **EDV3_Ch0.25NOx**, EDGAR-HTAP v3 with 75% reduction of NOx emission in China.

**Table S16**. Comparison of relative $O_3$, $NO_2$, and Ox (= $NO_2$ + $O_3$) biases with perturbed emissions based on EDGAR-HTAP v3, which is (Model – Observation)/Observation in each city; Beijing (39.4-41.1N, 115.4-117.5E), Tianjin (38.55-40.25N, 116.7-118.1E), Chengdu (30.05-31.5N, 103-105E), Chongqing (28.15-32.25N, 105.3-110.2E), Shanghai (30.7-31.5N, 120.85-122E), Hangzhou (29.2-30.6N, 118.3-120.9E), Nanjing (31.2-32.65N, 118.35-119.25E), Guangzhou (22.55-24N, 112.9-114.05E), Shenzhen (22.4-22.9N, 113.7-114.65E), SMA (37.2-37.8N, 126.5-127.3E), Wuhan (29.95-31.4N, 113.65-115.1E), and Xian (33.65-34.75N, 107.65-109.9E).

| | Emissions | Beijing | Tianjin | Chengdu | Chongqing | Shanghai | Hangzhou | Nanjing | Guangzhou | Shenzhen | SMA[1)] | Wuhan | Xian |
|---|---|---|---|---|---|---|---|---|---|---|---|---|---|
| $O_3$ bias (%) | **EDV3** | -6% | -9% | 55% | 68% | -24% | 27% | -13% | 15% | 16% | -12% | -1% | 34% |
| | **C1** | 39% | 36% | 86% | 107% | 20% | 81% | 36% | 51% | 38% | 19% | 47% | 69% |
| | **C2** | 39% | 36% | 86% | 107% | 19% | 81% | 35% | 51% | 38% | 6% | 46% | 69% |
| | **C3** | -5% | -8% | 55% | 68% | -23% | 28% | -13% | 15% | 17% | 0% | -1% | 34% |
| | **C4** | 22% | 26% | 48% | 70% | 16% | 53% | 28% | 49% | 42% | -14% | 31% | 49% |
| | **C5** | -32% | -33% | 38% | 48% | -45% | -4% | -37% | -4% | 4% | -21% | -25% | 16% |
| | **C6** | 5% | 8% | 38% | 57% | -4% | 33% | 7% | 33% | 33% | -20% | 12% | 37% |
| | **C7** | 18% | 29% | 27% | 50% | 27% | 45% | 37% | 56% | 49% | -20% | 30% | 41% |
| $NO_2$ bias (%) | **EDV3** | 22% | 30% | -23% | 6% | 112% | 28% | 126% | 64% | 73% | -2% | 103% | -7% |
| | **C1** | 5% | 19% | -31% | -1% | 108% | 7% | 122% | 55% | 68% | -4% | 96% | -15% |
| | **C2** | 5% | 19% | -31% | -1% | 108% | 7% | 122% | 55% | 68% | 0% | 96% | -15% |
| | **C3** | 22% | 30% | -23% | 6% | 112% | 28% | 126% | 64% | 73% | -5% | 103% | -7% |
| | **C4** | -47% | -39% | -63% | -48% | 11% | -44% | 21% | -16% | -10% | -3% | 2% | -56% |
| | **C5** | 30% | 33% | -18% | 8% | 109% | 39% | 122% | 67% | 75% | -3% | 102% | -4% |
| | **C6** | -41% | -35% | -61% | -45% | 17% | -37% | 26% | -9% | -8% | -4% | 7% | -53% |
| | **C7** | -76% | -72% | -82% | -74% | -49% | -75% | -42% | -61% | -56% | -5% | -51% | -79% |
| Ox bias (%) | **EDV3** | 1% | 4% | 36% | 48% | 17% | 28% | 31% | 33% | 33% | -7% | 30% | 20% |
| | **C1** | 30% | 31% | 57% | 73% | 46% | 57% | 63% | 52% | 47% | 9% | 62% | 40% |
| | **C2** | 30% | 31% | 57% | 73% | 46% | 56% | 63% | 52% | 47% | 4% | 62% | 40% |
| | **C3** | 2% | 4% | 36% | 48% | 17% | 28% | 31% | 33% | 33% | -1% | 30% | 20% |
| | **C4** | 3% | 5% | 21% | 33% | 14% | 21% | 26% | 24% | 27% | -8% | 23% | 12% |
| | **C5** | -16% | -12% | 25% | 35% | 1% | 11% | 13% | 23% | 25% | -13% | 13% | 9% |
| | **C6** | -8% | -6% | 14% | 25% | 2% | 10% | 13% | 17% | 21% | -12% | 11% | 5% |
| | **C7** | -8% | -4% | 1% | 11% | 4% | 5% | 12% | 12% | 18% | -13% | 7% | -1% |

[1)]**Seoul Metropolitan Area**
**C1**: **EDV3_ChKo2**, EDGAR-HTAP v3 with double CO and VOC emissions in China and South Korea.
**C2**: **EDV3_Ch2**, EDGAR-HTAP v3 with double CO and VOC emissions in China.
**C3**: **EDV3_Ko2**, EDGAR-HTAP v3 with double CO and VOC emissions in South Korea.
**C4**: **EDV3_Ch0.5NOx**, EDGAR-HTAP v3 with 50% reduction of NOx emission in China.
**C5**: **EDV3_Ch0.5VOC**, EDGAR-HTAP v3 with 50% reduction of VOC emission in China.
**C6**: **EDV3_Ch0.5NOxVOC**, EDGAR-HTAP v3 with 50% reductions of NOx and VOC emissions in China.
**C7**: **EDV3_Ch0.25NOx**, EDGAR-HTAP v3 with 75% reduction of NOx emission in China.

**Table S17**. Same as **Table S16** except absolute biases (Model-Observation, unit=ppb).

| | Emissions | Beijing | Tianjin | Chengdu | Chongqing | Shanghai | Hangzhou | Nanjing | Guangzhou | Shenzhen | SMA[1)] | Wuhan | Xian |
|---|---|---|---|---|---|---|---|---|---|---|---|---|---|
| **$O_3$ bias (ppb)** | **EDV3** | -2.8 | -3.9 | 23.1 | 21.2 | -10.1 | 9.2 | -4.6 | 3.9 | 4.9 | -4.3 | -0.4 | 12.1 |
| | **C1** | 18.9 | 15.5 | 35.7 | 33.4 | 8.4 | 27.4 | 12.3 | 13.6 | 11.3 | 6.9 | 16.7 | 24.7 |
| | **C2** | 18.7 | 15.2 | 35.7 | 33.4 | 8.0 | 27.2 | 12.2 | 13.5 | 11.2 | 2.3 | 16.7 | 24.7 |
| | **C3** | -2.6 | -3.5 | 23.1 | 21.2 | -9.7 | 9.5 | -4.4 | 4.0 | 5.0 | 0.2 | -0.3 | 12.2 |
| | **C4** | 10.4 | 11.1 | 19.9 | 21.8 | 6.8 | 18.1 | 9.8 | 13.0 | 12.5 | -5.1 | 11.1 | 17.6 |
| | **C5** | -15.5 | -14.0 | 16.0 | 15.0 | -18.9 | -1.4 | -12.7 | -1.2 | 1.3 | -7.8 | -8.9 | 5.7 |
| | **C6** | 2.2 | 3.6 | 15.9 | 17.8 | -1.8 | 11.1 | 2.3 | 8.8 | 9.9 | -7.3 | 4.2 | 13.1 |
| | **C7** | 8.5 | 12.4 | 11.4 | 15.7 | 11.3 | 15.0 | 12.9 | 15.0 | 14.5 | -7.4 | 10.7 | 14.7 |
| **$NO_2$ bias (ppb)** | **EDV3** | 3.9 | 6.0 | -3.1 | 0.9 | 20.1 | 4.9 | 20.0 | 10.3 | 8.9 | -0.5 | 15.4 | -1.4 |
| | **C1** | 0.9 | 4.0 | -4.2 | -0.2 | 19.3 | 1.3 | 19.4 | 8.9 | 8.4 | -1.2 | 14.3 | -2.9 |
| | **C2** | 0.9 | 4.0 | -4.2 | -0.2 | 19.3 | 1.3 | 19.4 | 8.9 | 8.4 | 0.0 | 14.3 | -2.9 |
| | **C3** | 3.9 | 6.0 | -3.1 | 0.9 | 20.1 | 4.8 | 20.0 | 10.3 | 8.9 | -1.5 | 15.4 | -1.4 |
| | **C4** | -8.3 | -8.0 | -8.5 | -6.9 | 1.9 | -7.5 | 3.3 | -2.5 | -1.3 | -1.0 | 0.4 | -11.0 |
| | **C5** | 5.4 | 6.8 | -2.5 | 1.2 | 19.6 | 6.7 | 19.3 | 10.9 | 9.1 | -1.1 | 15.3 | -0.9 |
| | **C6** | -7.3 | -7.1 | -8.2 | -6.6 | 3.1 | -6.4 | 4.1 | -1.5 | -1.0 | -1.4 | 1.0 | -10.4 |
| | **C7** | -13.5 | -14.7 | -11.0 | -10.7 | -8.8 | -12.8 | -6.6 | -9.8 | -6.9 | -1.6 | -7.6 | -15.5 |
| **Ox bias (ppb)** | **EDV3** | 1.0 | 2.2 | 20.1 | 21.9 | 10.0 | 14.2 | 15.4 | 14.1 | 13.8 | -4.6 | 15.2 | 10.8 |
| | **C1** | 19.7 | 19.5 | 31.6 | 33.1 | 27.7 | 28.7 | 31.7 | 22.3 | 19.7 | 6.0 | 31.3 | 21.9 |
| | **C2** | 19.5 | 19.2 | 31.6 | 33.1 | 27.3 | 28.6 | 31.5 | 22.3 | 19.6 | 2.6 | 31.2 | 21.9 |
| | **C3** | 1.2 | 2.5 | 20.1 | 22.0 | 10.5 | 14.4 | 15.6 | 14.2 | 13.9 | -1.0 | 15.3 | 10.8 |
| | **C4** | 1.9 | 3.2 | 11.4 | 14.9 | 8.7 | 10.7 | 13.0 | 10.4 | 11.3 | -5.8 | 11.7 | 6.7 |
| | **C5** | -10.2 | -7.2 | 13.5 | 16.1 | 0.7 | 5.4 | 6.6 | 9.6 | 10.4 | -8.6 | 6.6 | 4.9 |
| | **C6** | -5.3 | -3.5 | 7.7 | 11.2 | 1.2 | 4.8 | 6.4 | 7.2 | 8.9 | -8.4 | 5.5 | 2.7 |
| | **C7** | -5.2 | -2.2 | 0.4 | 5.0 | 2.5 | 2.3 | 6.2 | 5.1 | 7.7 | -8.8 | 3.5 | -0.7 |

[1)]**Seoul Metropolitan Area**

**C1**: **EDV3_ChKo2**, EDGAR-HTAP v3 with double CO and VOC emissions in China and South Korea.
**C2**: **EDV3_Ch2**, EDGAR-HTAP v3 with double CO and VOC emissions in China.
**C3**: **EDV3_Ko2**, EDGAR-HTAP v3 with double CO and VOC emissions in South Korea.
**C4**: **EDV3_Ch0.5NOx**, EDGAR-HTAP v3 with 50% reduction of NOx emission in China.
**C5**: **EDV3_Ch0.5VOC**, EDGAR-HTAP v3 with 50% reduction of VOC emission in China.
**C6**: **EDV3_Ch0.5NOxVOC**, EDGAR-HTAP v3 with 50% reductions of NOx and VOC emissions in China.
**C7**: **EDV3_Ch0.25NOx**, EDGAR-HTAP v3 with 75% reduction of NOx emission in China.

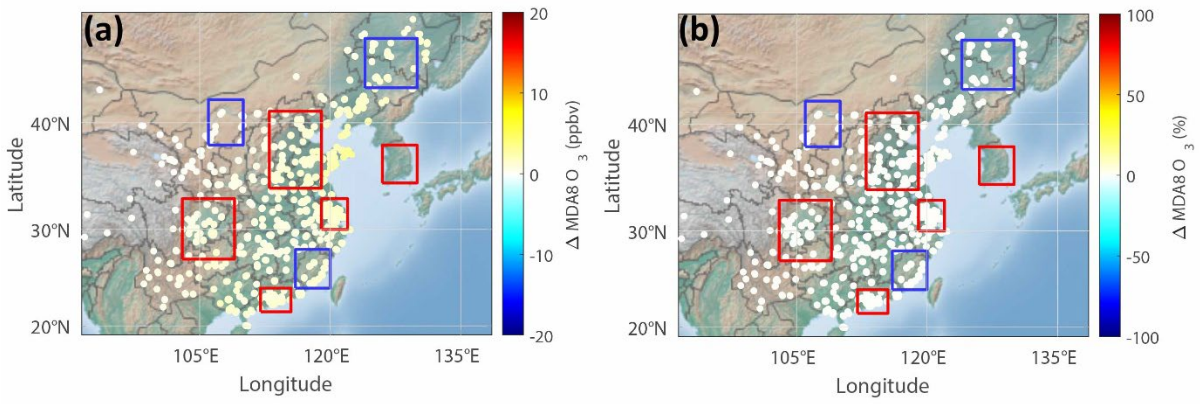


**Figure S1**. Comparison of the model surface MDA8 $O_3$ using EDGAR-HTAP v3 between with (EDV3_Fire) and without fire emissions (EDV3) at China surface observation sites during the whole campaign period (KORUS-AQ). (a) and (b) are absolute and relative differences between EDV3 and EDV3_Fire (EDV3_Fire – EDV3) respectively. The boxes represent Northern China (NOC, 38-42˚N/106-110˚E), Sichuan-Chongqing-Guizhou (SCG, 27-33˚N/103-109˚E), Pearl River Delta (PRD, 21.5-24˚N/112-115.5˚E), Southeastern China (SEC, 24-28˚N/116-120˚E), Yangtze River Delta (YRD, 30-33˚N/119-122˚E), South Korea (KOR, 34.5-38˚N/126-130˚E), North China Plain (NCP, 34-41˚N/113-119˚E), and Northeastern China (NEC, 43-47˚N/124-130˚E). NOC, NEC, and SEC are denoted by blue boxes (non-urban). NCP, SCG, PRD, YRD, and KOR are denoted by red boxes (urban).

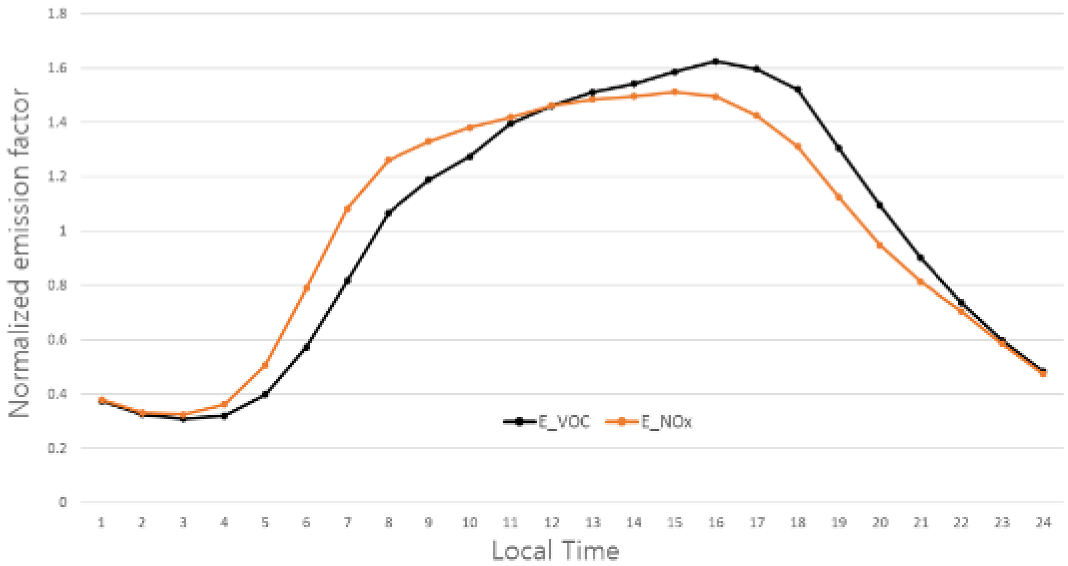


**Figure S2**. Diurnal emission factors of VOC and $NO_x$.

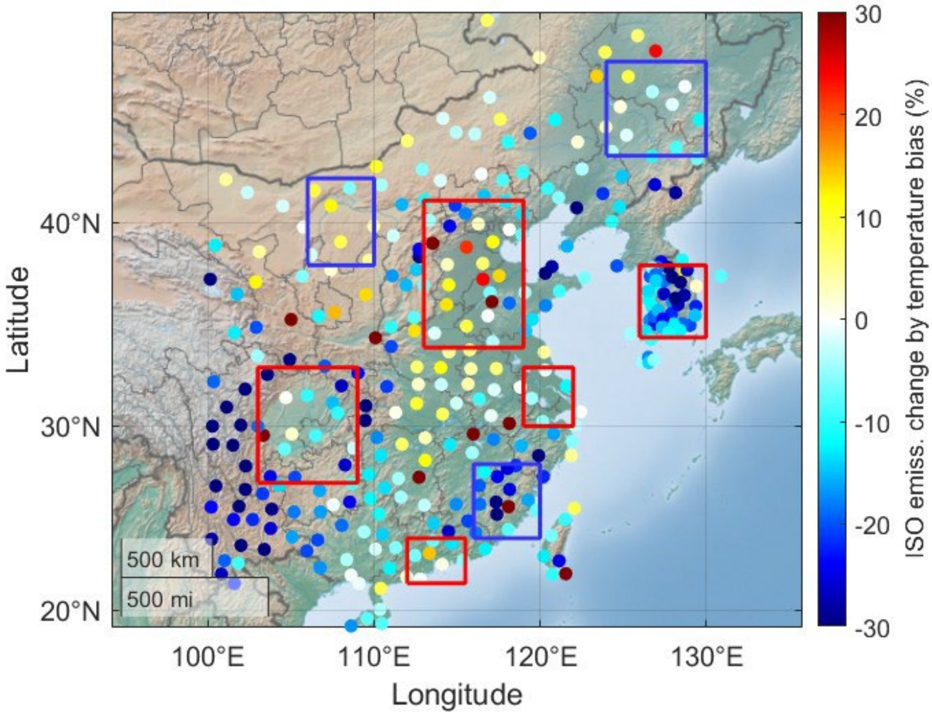


**Figure S3**. Relative ISO (isoprene) emission change from the temperature bias at the surface (unit = %).

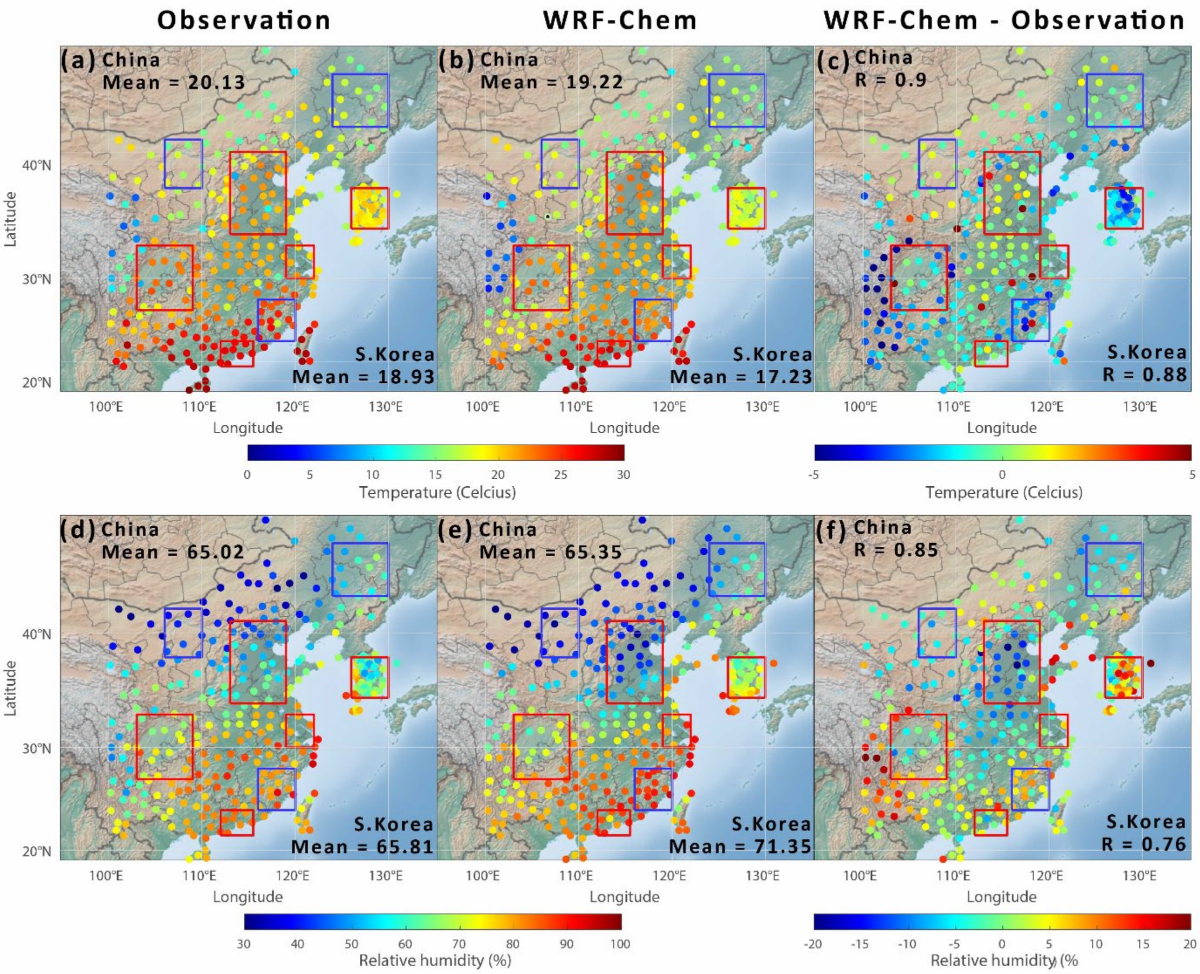


**Figure S4**. Averaged surface temperature (unit: ˚C) and relative humidity (unit: %) from (a, d) ground-based observations (SYNOP) and (b, e) the weather research and forecast (WRF) model coupled with chemistry (WRF-Chem) from 1st May to 10th June for each station and countries. The differences and correlation coefficients between averaged observations and WRF-Chem are shown (c, f).

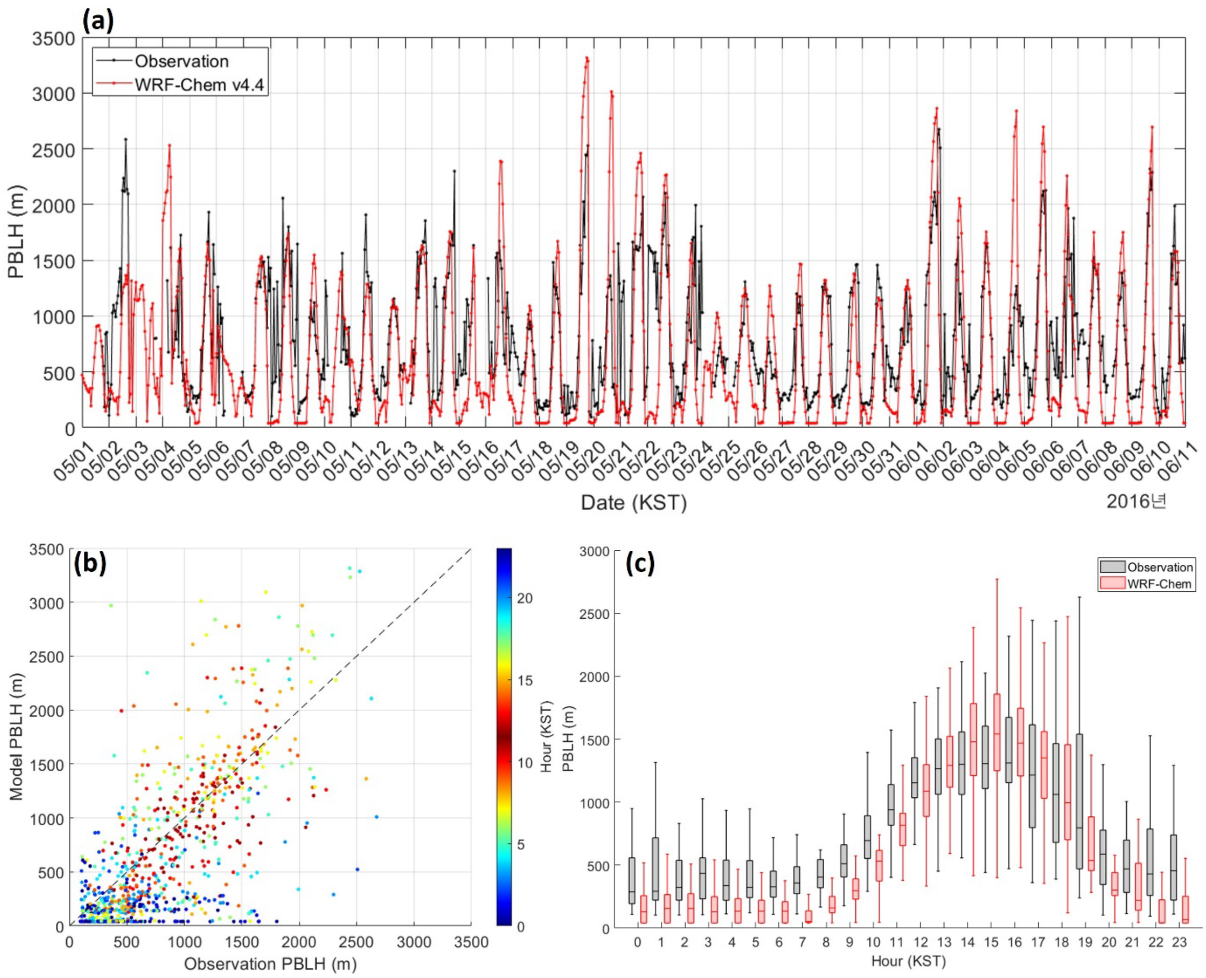


**Figure S5**. Comparison of PBL heights derived from the ceilometer at Yonsei University (37.564˚N, 126.935˚E) with the WRF-Chem results during the KORUS-AQ campaign period: (a) time series of planetary boundary layer height from ceilometer and WRF-Chem (unit = m), (b) scatter plot of which x axis is ceilometer and y axis is WRF-Chem PBL height, (c) comparison of diurnal variations of PBL heights from ceilometer (grey) and WRF-Chem (red) with box whisker plot.

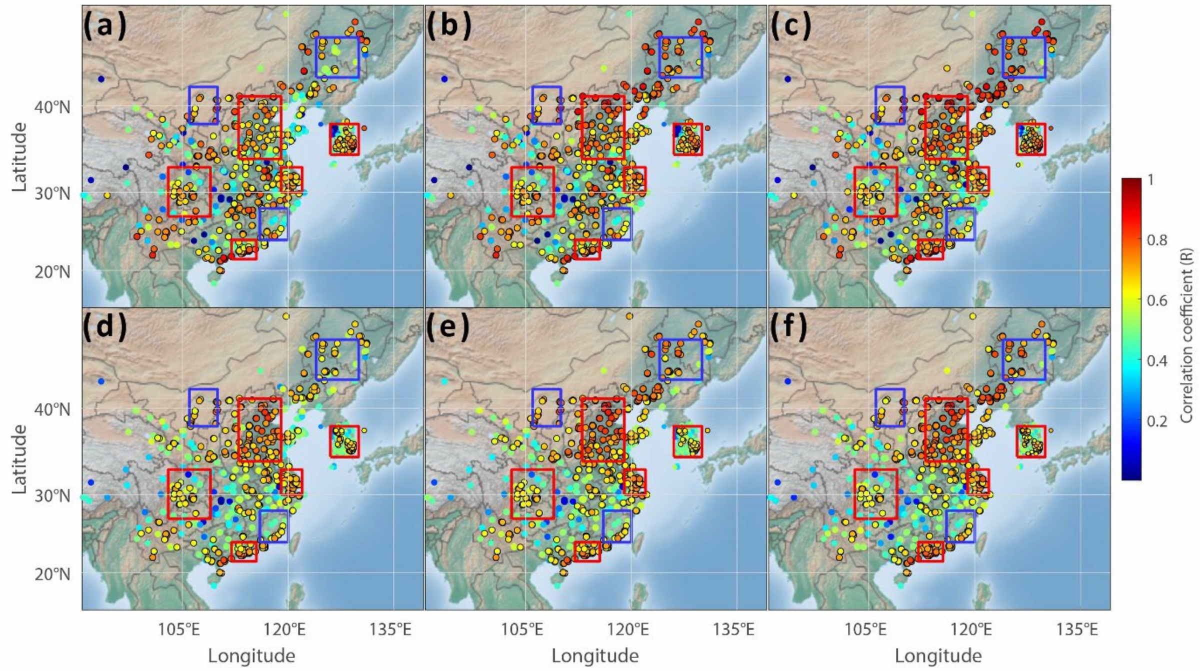


**Figure S6**. Correlation coefficient (R) between observed and simulated (a-c) MDA8 $O_3$ and (d-f) hourly $O_3$ with (a, d) EDV2, (b, e) EDV3, and (c, f) KOV5 emissions. The observation sites with R greater than 0.6 are indicated by a black circle.

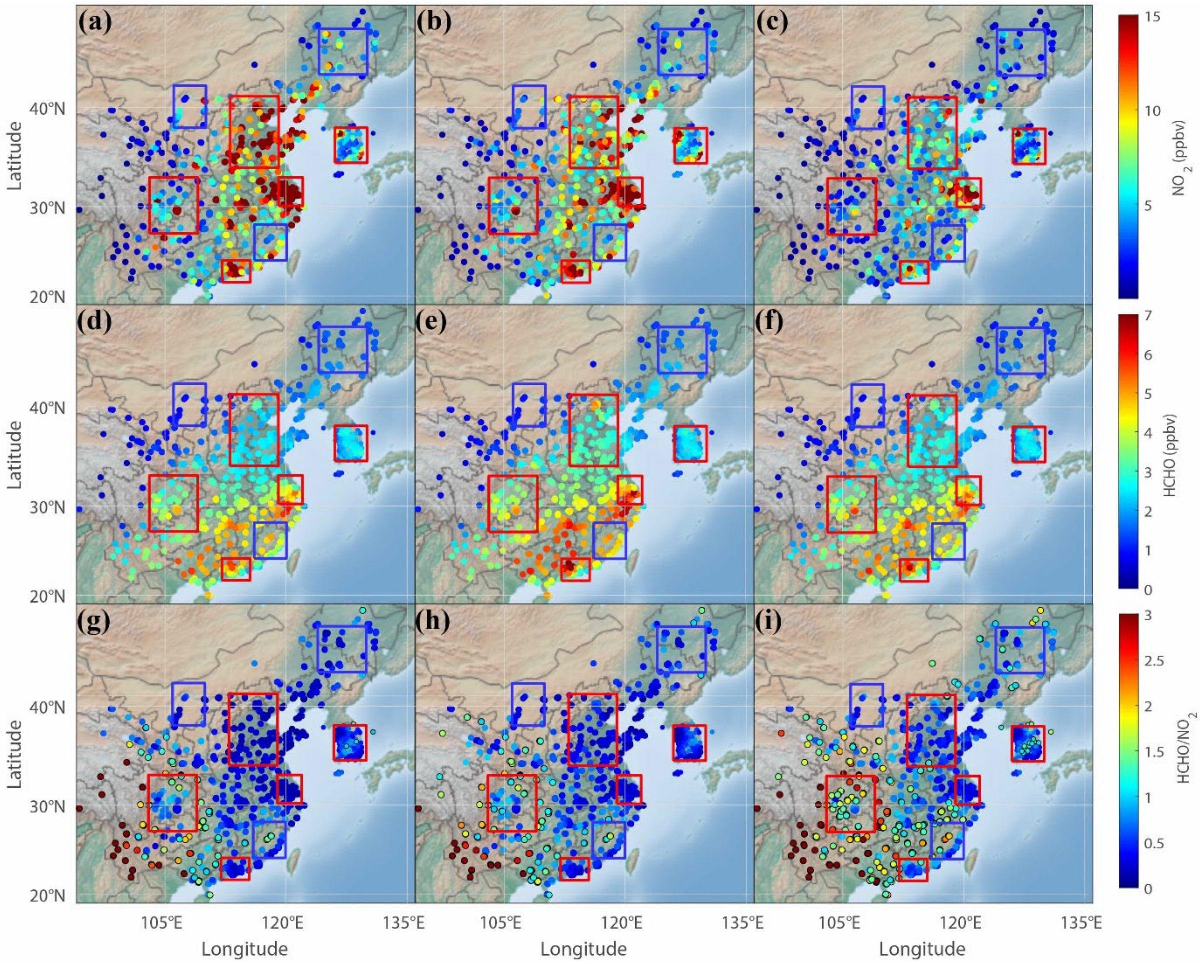


**Figure S7**. Simulated surface (a-c) $NO_2$ and (d-f) HCHO concentrations and (g-i) HCHO to $NO_2$ ratio (FNR) with (a, d, g) EDV2, (b, e, h) EDV3, and (c, f, i) KOV5 emissions for 14-16 LST. FNR greater than 1 is marked with black circles. The simulated $NO_2$, HCHO, and FNR are linearly interpolated to ground-based observation sites.

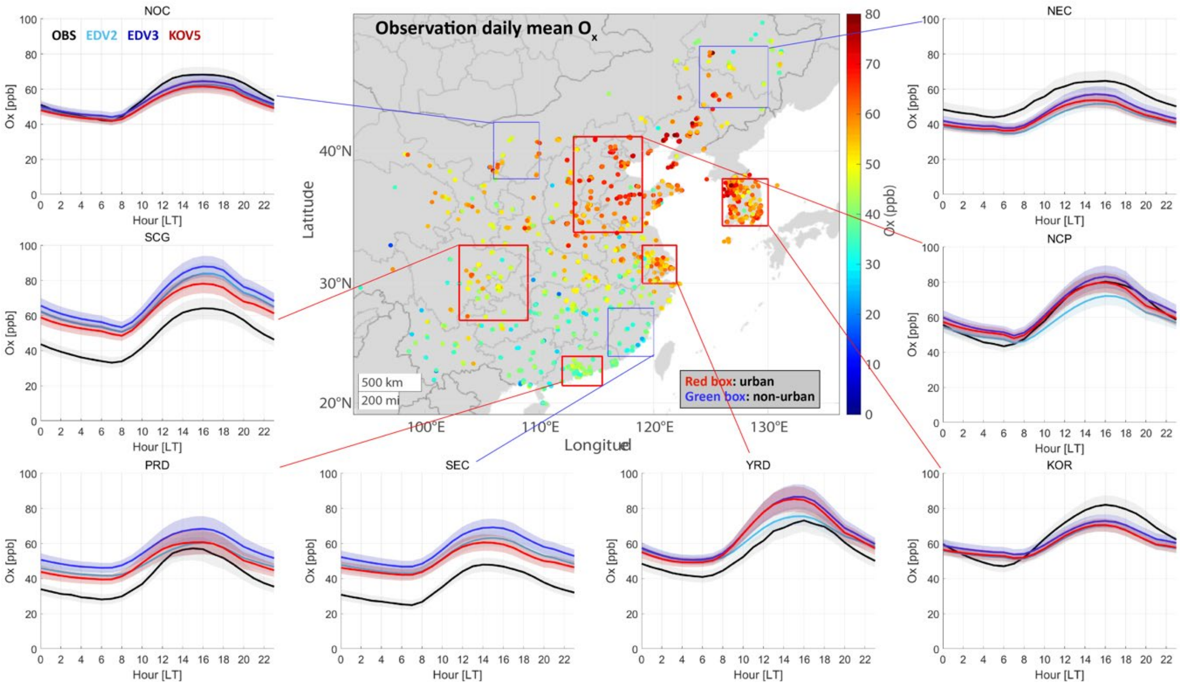


**Figure S8**. The same as **Figure 3** except Ox (= $NO_2$ + $O_3$).

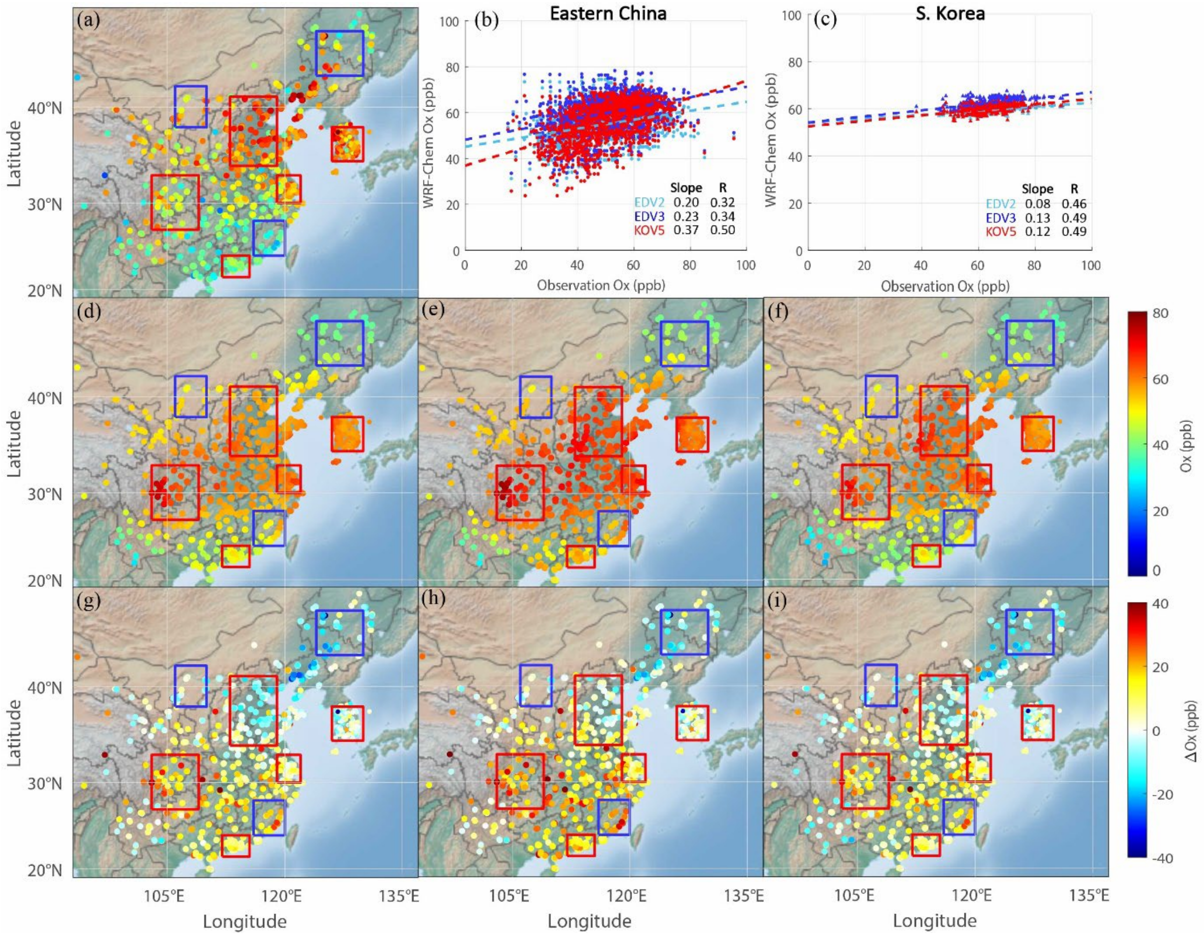


**Figure S9.** The same as **Figure 4** except Ox (= $NO_2$ + $O_3$).

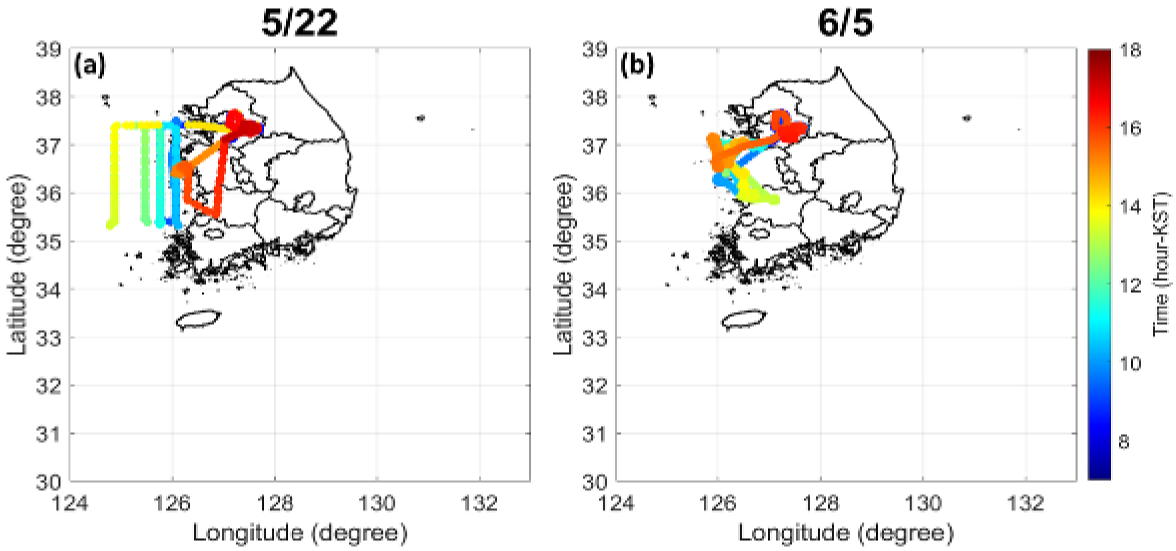


**Figure S10**. The DC-8 flight tracks on the 22nd May and 5th June.

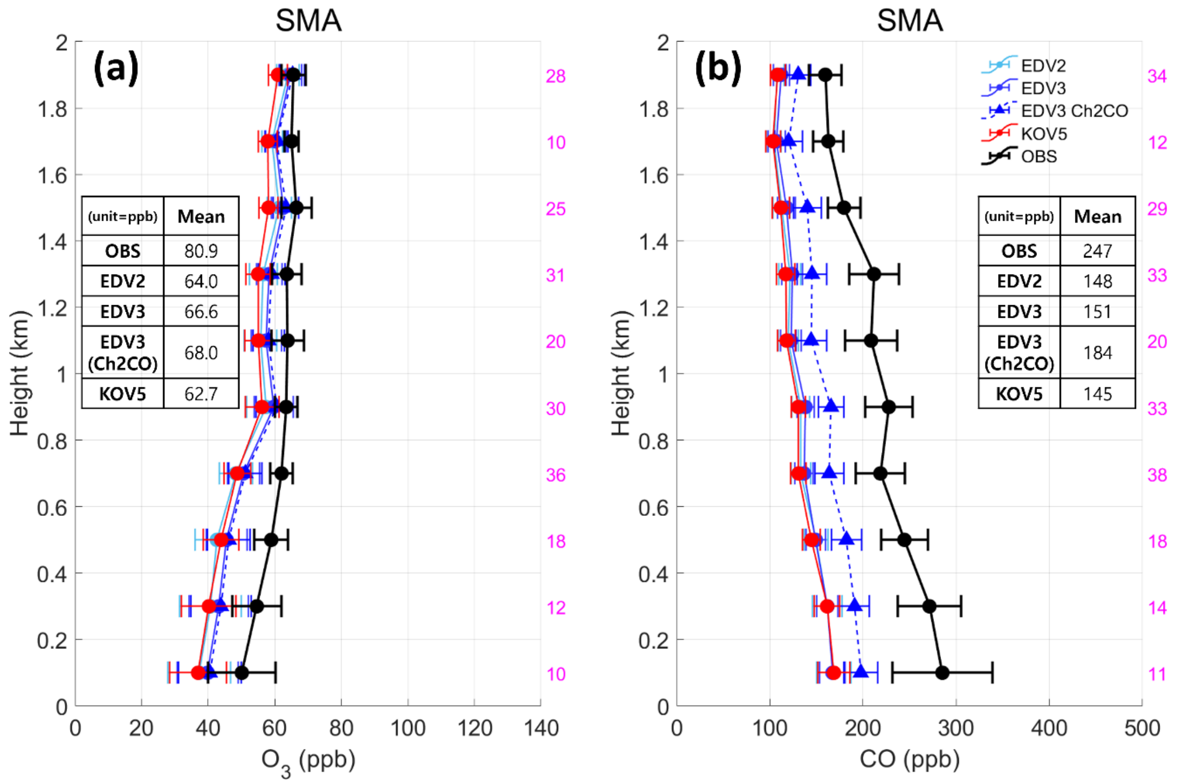


**Figure S11**. Vertically averaged (a) $O_3$ and (b) CO from DC-8 (black), EDV2 (sky blue), EDV3 (blue), EDV3 with double CO emission in China (EDV3 Ch2CO) (blue dashed) and KOV5 (red) 3 in SMA under 2 km height above ground level. The 1/2 of standard deviations are represented with black whiskers in each 200m layer. The sample number is presented with magenta color on the right side of the plots.

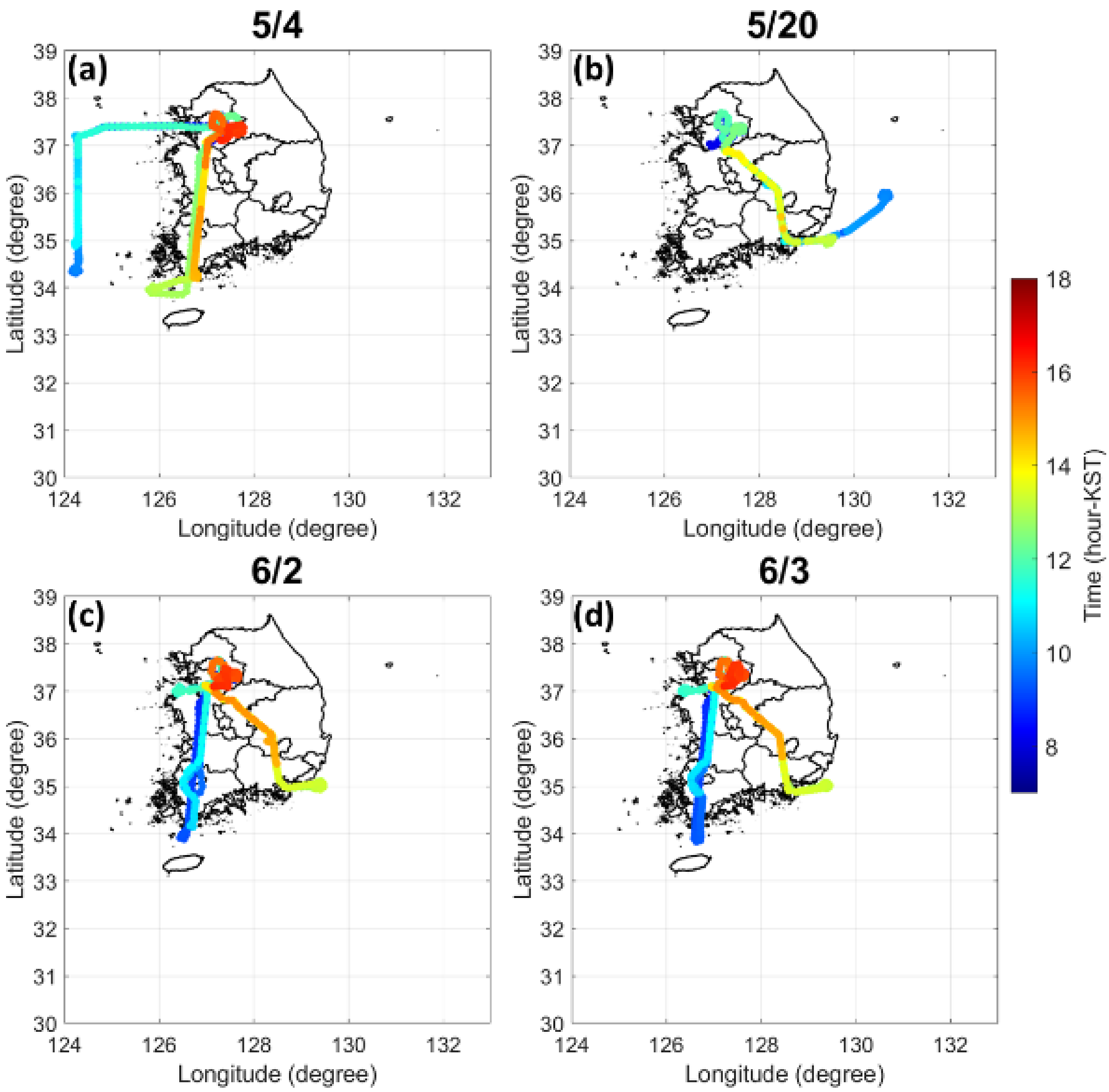


**Figure S12**. The DC-8 flight tracks on the 4th, 20th May and 2nd, 3rd June (Local case).

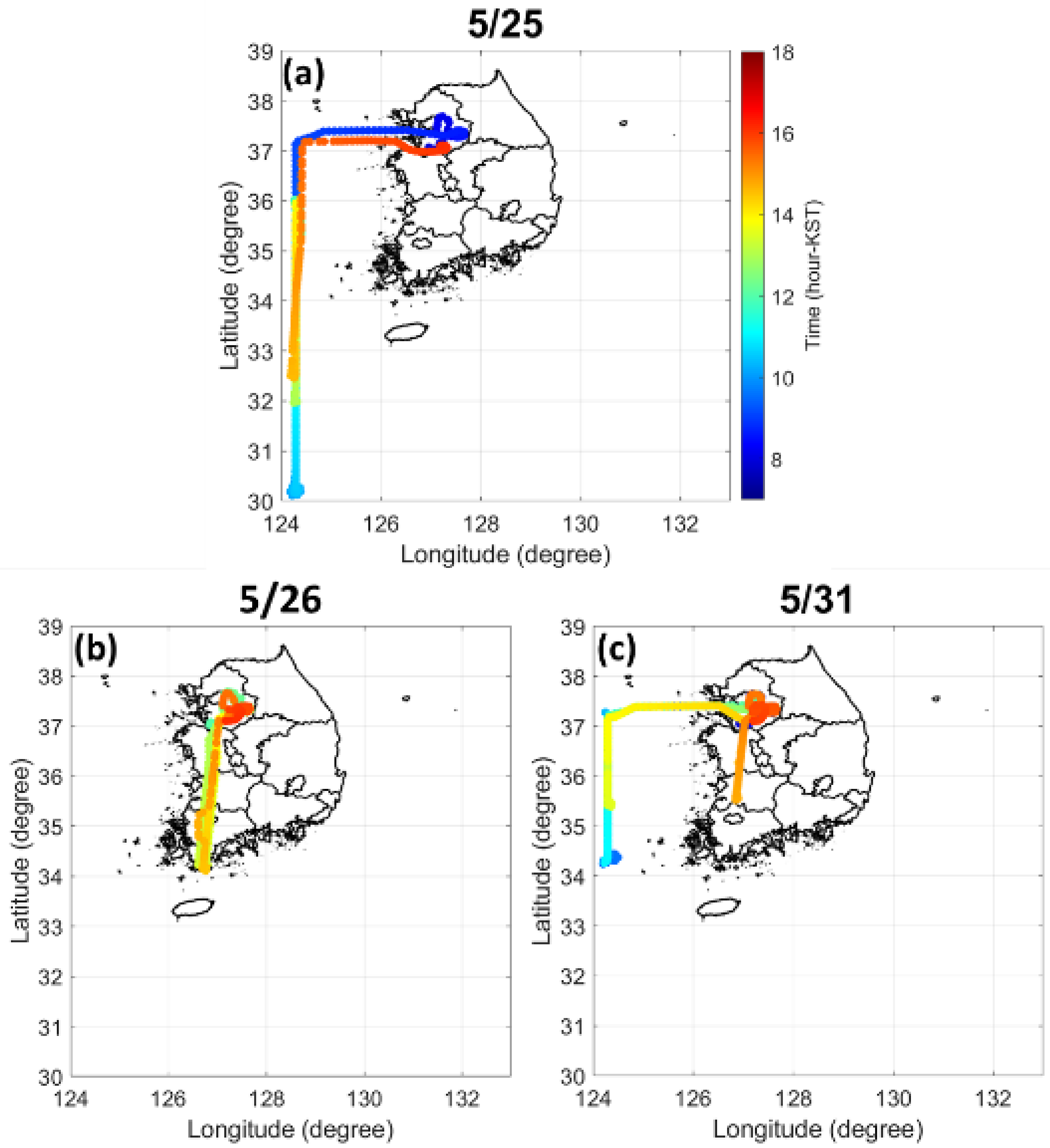


**Figure S13**. The DC-8 flight tracks on the 22nd, 27th, 31st May (Transport case).

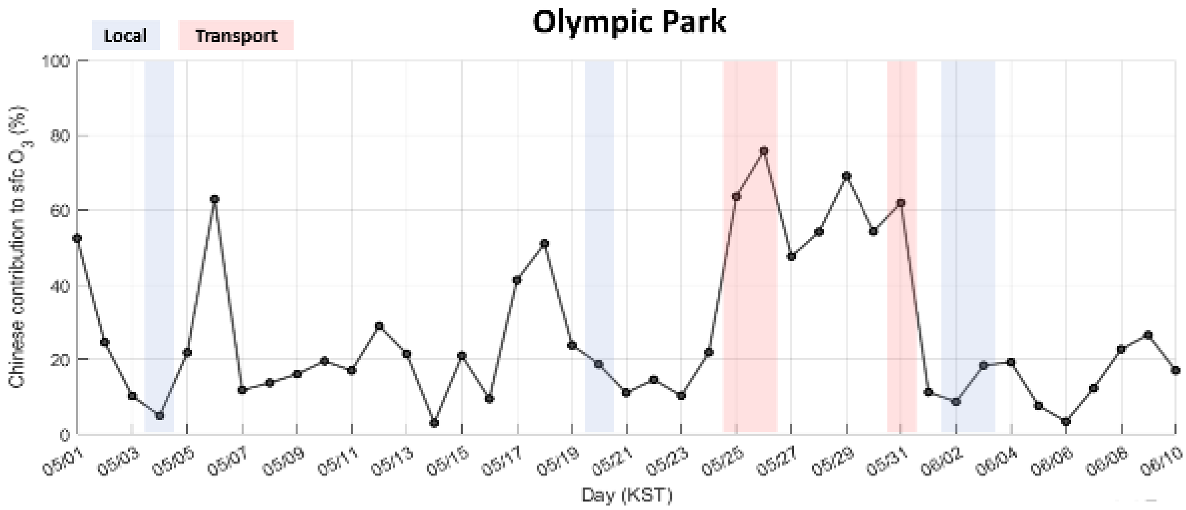


**Figure S14.** The contribution of Chinese emissions (%) to daily surface $O_3$ concentrations at Olympic Park obtained from the EDV3 simulations with/without Chinese anthropogenic emissions.

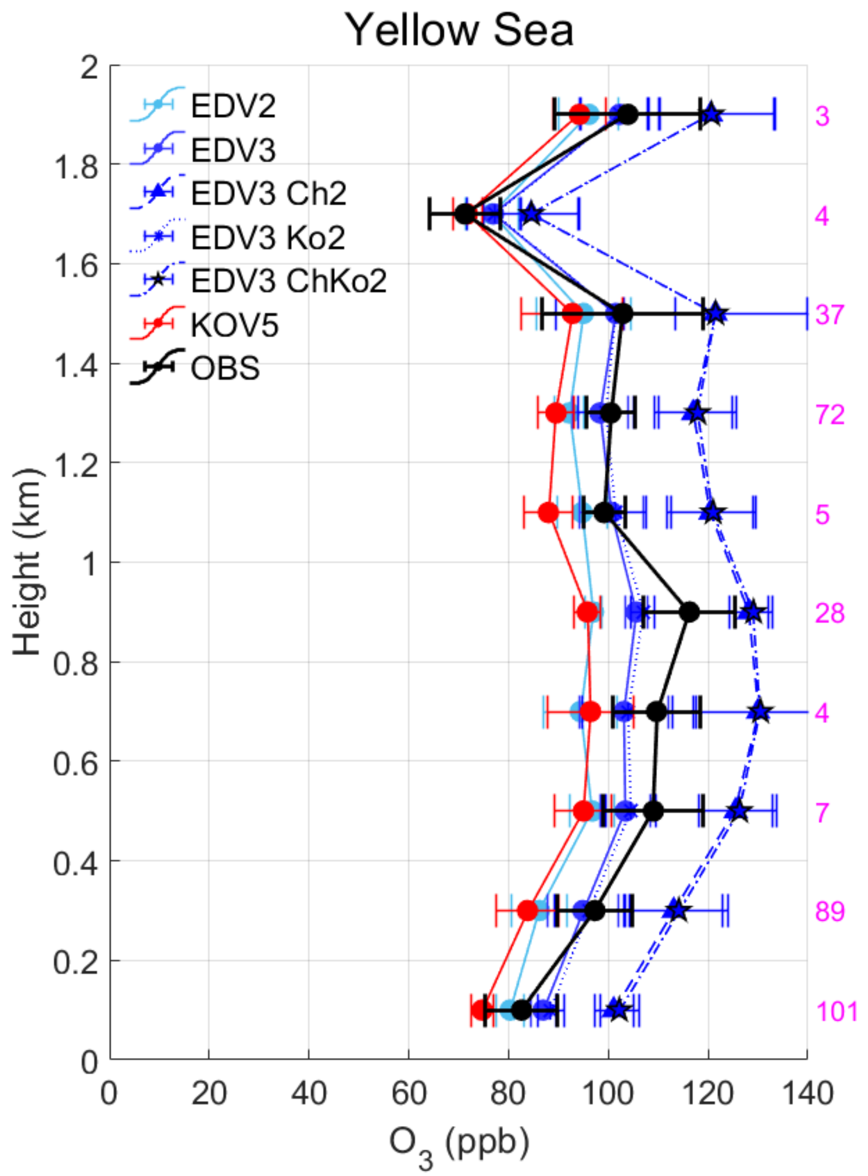


**Figure S15**. Vertically averaged $O_3$ from DC-8 (black), EDV2 (sky blue), EDV3 (blue), KOV5 (red), EDV3 with doubling Chinese CO and VOC emissions (dashed blue), EDV3 with doubling Korean CO and VOC emissions (dotted blue), and EDV3 with doubling Chinese and Korean CO and VOC emissions (dotted dashed blue) in Yellow Sea under 2 km height above ground level. The 1/2 of standard deviations are represented with whiskers in each 200m layer, The sample number is presented with magenta color on the right side of the plots.

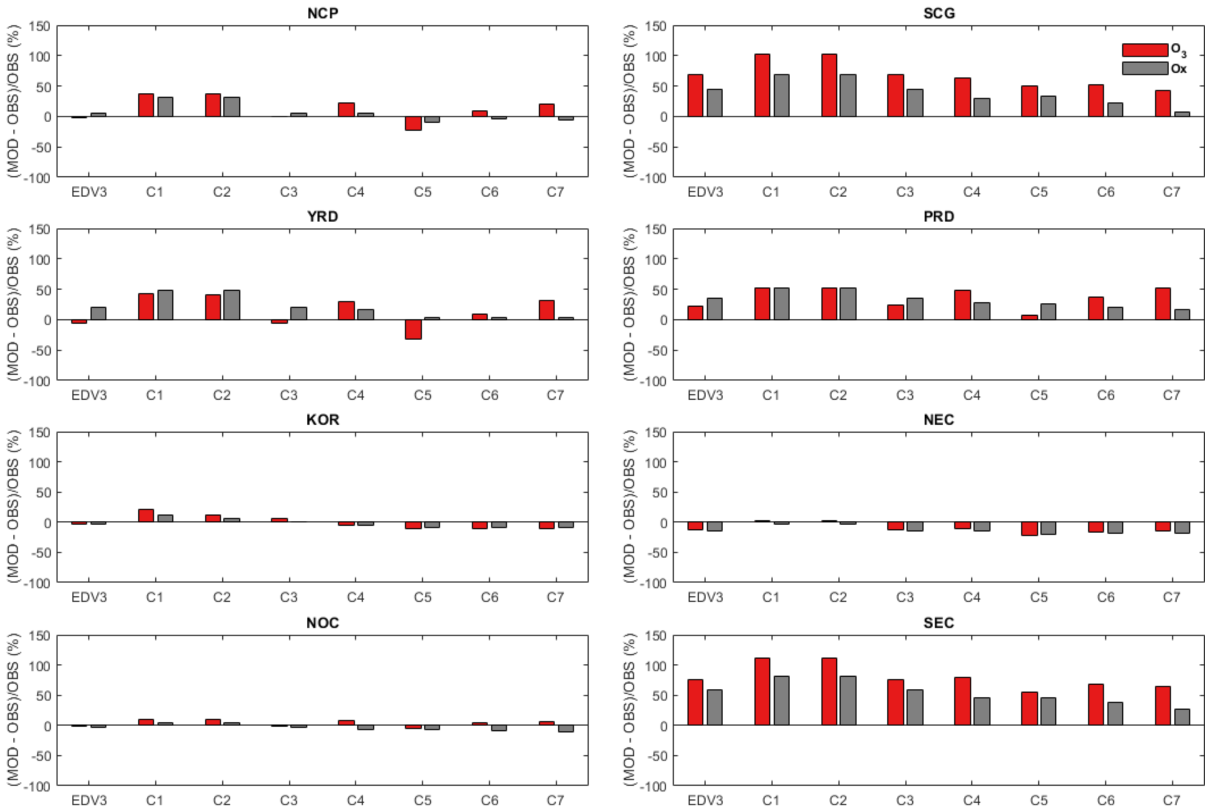


**Figure S16**. Same as **Figure 14** except that $NO_2$ is changed to Ox (= $NO_2$ + $O_3$).

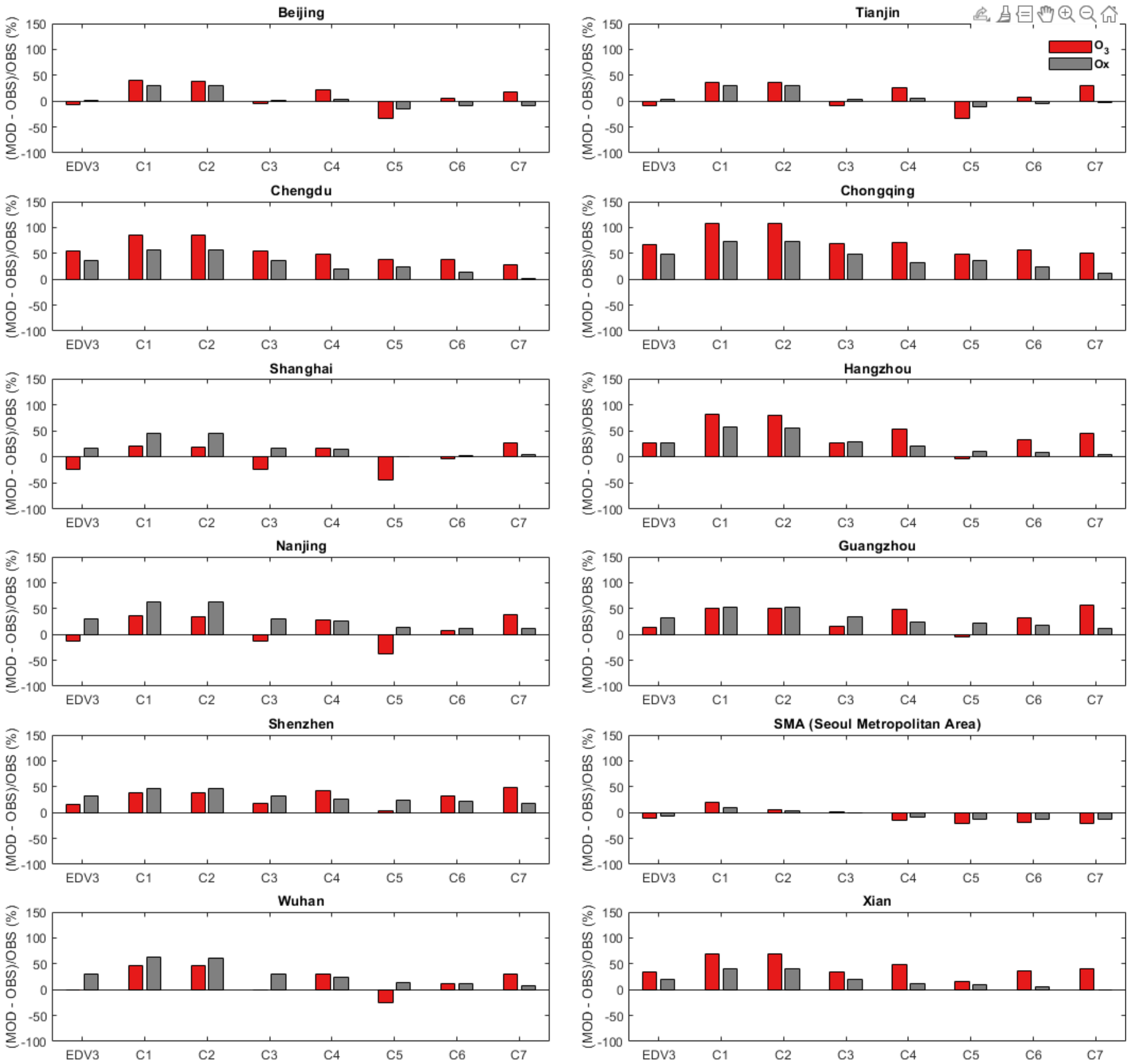


**Figure S17**. Same as **Figure 15** except that $NO_2$ is changed to Ox (= $NO_2$ + $O_3$).

## References


Ackermann, I. J., Hass, H., Memmesheimer, M., Ebel, A., Binkowski, F. S., and Shankar, U.: Modal aerosol dynamics model for Europe: Development and first applications, *Atmos. Environ.*, 32, 2981-2999, https://doi.org/10.1016/S1352-2310(98)00006-5, 1998.

Ahmadov, R., McKeen, S. A., Robinson, A. L., Bahreini, R., Middlebrook, A. M., de Gouw, J. A., Meagher, J., Hsie, E.-Y., Edgerton, E., Shaw, S., and Trainer, M.: A volatility basis set model for summertime secondary organic aerosols over the eastern United States in 2006, *J. Geophys. Res. Atmos.*, 117, D06301, https://doi.org/10.1029/2011JD016831, 2012.

Carter, W. P.: Documentation of the SAPRC-99 chemical mechanism for VOC reactivity assessment, Contract, 92, 95–308, https://intra.engr.ucr.edu/~carter/pubs/s99doc.pdf (last access: 9 June 2023), 2000.

Chen, S.-H. and Sun, W.-Y.: A one-dimensional time dependent cloud model, *J. Meteorol. Soc. Japan*, 80, 99-118, https://doi.org/10.2151/jmsj.80.99, 2002.

Emmons, L. K., Walters, S., Hess, P. G., Lamarque, J.-F., Pfister, G. G., Fillmore, D., Granier, C., Guenther, A., Kinnison, D., Laepple, T., Orlando, J., Tie, X., Tyndall, G., Wiedinmyer, C., Baughcum, S. L., and Kloster, S.: Description and evaluation of the Model for Ozone and Related chemical Tracers, version4(MOZART-4), *Geosci. Model Dev.*, 3, 43-67, https://doi.org/10.5194/gmd-3-43-2010, 2010.

Grell, G. A. and Dévényi, D.: A generalized approach to parameterizing convection combining ensemble and data assimilation techniques, *Geophys. Res. Lett.*, 29, 38-1-38-4, https://doi.org/10.1029/2002GL015311, 2002.

Grell, G. A.: Prognostic evaluation of assumptions used by cumulus parameterizations, *Mon. Weather Rev.*, 121, 764-787, https://doi.org/10.1175/1520-0493(1993)121<0764:PEOAUB>2.0.CO;2, 1993.

Hong, S.-Y. and Noh, Y.: A new vertical diffusion package with an explicit treatment of entrainment processes, *Mon. Weather Rev.*, 134, 2318–2341, https://doi.org/10.1175/MWR3199.1. 2006.

Lu, K. D., Hofzumahaus, A., Holland, F., Bohn, B., Brauers, T., Fuchs, H., Hu, M., Häseler, R., Kita, K., Kondo, Y., Li, X., Lou, S. R., Oebel, A., Shao, M., Zheng, J. M., Wahner, A., Zhu, T., Zhang, T. H., and Rohrer, F.: Missing OH source in a suburban environment near Beijing: observed and modelled OH and $HO_2$ concentrations in summer 2006, *Atmos. Chem. Phys.*, 13, 1057-1080, doi.org/10.5194/acp-13-1057-2013, 2013.

Madronich, S.: Photodissociation in the Atmosphere, 1, actinic flux and the effects of ground reflections and clouds, *J. Geophys. Res. Atmos.*, 92, 9740–9752. https://doi.org/10.1029/JD092iD08p09740, 1987.

Stockwell, W. R., Kirchner, F., and Kuhn, M.: A new mechanism for regional atmospheric chemistry modeling, *J. Geophys. Res. Atmos.*, 102, 25847-25879, https://doi.org/10.1029/97JD00849, 1997.

Tewari, M., F. Chen, W. Wang, J. Dudhia, M. A. LeMone, K. Mitchell, M. Ek, G. Gayno, J. Wegiel, and Cuenca, R. H.: Implementation and verification of the unified NOAH land surface model in the WRF model, *20th conference on weather analysis and forecasting/16th conference on numerical weather prediction*, pp. 11–15, 2004.